Structures 62 (2024) 106160

Contents lists available at ScienceDirect

Structures

journal homepage: www.elsevier.com/locate/structures

A comprehensive study on the impact of nano-silica and ground granulated blast furnace slag on high strength concrete characteristics: RSM modeling and optimization

Naraindas Bheel [a,*], Ahsan Waqar [a], Dorin Radu [b], Omrane Benjeddou [c], Mamdooh Alwetaishi [d], Hamad R. Almujibah [d]

[a] Department of Civil and Environmental Engineering, Universiti Teknologi PETRONAS, Bandar Seri Iskandar, Tronoh, Perak 32610, Malaysia
[b] Faculty of Civil Engineering, Transilvania University of Brașov, 500156 Turnului street 5, Brașov, Romania
[c] Department of Civil Engineering, College of Engineering, Prince Sattam Bin Abdulaziz University, Alkharj 16273, Saudi Arabia
[d] Department of Civil Engineering, College of Engineering, Taif University, P.O. Box 11099, Taif 21944, Saudi Arabia

ARTICLE INFO

Keywords:
High strength concrete
Nanao-Silica
GGBFS
Mechanical Properties
RSM modelling and Optimizations

ABSTRACT

In light of the global climate change crisis, the imperative to mitigate carbon emission sources is growing in significance. Cement is a notable contributor to greenhouse gas emissions (GHG) due to its industrial manufacturing process, which results in the release of 0.9 kg of GHG per kilogram produced. Therefore, to reduce GHG by using Ground granulated blast furnace slag (GGBFS) as a substitution for cement in high strength concrete (HSC). However, the use of nano silica (NS) as nanomaterial in HSC to improve the mechanical and durability characteristics of HSC. Besides, Response Surface Methodology (RSM) was adopted to assess the workability test (slump), compressive strength (CS), splitting tensile strength (STS), flexural strength (FS), modulus of elasticity and water absorption (WA) of HSC blended with 5–20% of GGBFS with an 5% increment and 1–4% of NS with an 1% increment as nanomaterial. CS outcomes were obtained at 7 days, 28 days, 90 days while STS, FS, MOE, and WA assessments were observed at 28 days. From experimental outcomes, Slump and WA were found to be reduced with the addition of GGBFS and NS rises in HSC. Moreover, the highest CS, STS, FS, and MOE were observed by 91.78 MPa, 5.25 MPa, 5.05 MPa, 46.06 GPa at 10% of GGBFS and 3% of NS together in HSC at 28 days respectively. Additionally, the embodied carbon was found to be decreasing with the addition of GGBFS and NS increases in HSC. Furthermore, response prediction models were developed and verified using ANOVA with a significance level of 95%. The R-Square values for the models ranged from 93 to 99.50%. It has been concluded that the use of 10% of GGBFS as replacement for cement and 3% of NS together in HSC is providing optimum outcomes therefore, it is recommended for construction industry.

1. Introduction

The most extensively used heterogeneous material in the global construction industry is concrete. The composition of concrete is of great importance as it grants the material a unique amalgamation of advantageous characteristics, including strength, durability, and versatility [1]. As a result, concrete is an essential and extensively utilized material across multiple fields within the construction industry. Concrete combines cement, water, and aggregates of various sizes according to the requirements for strength [2]. Hi et al. [3] stated that, although all the ingredients are important for concrete, cement has always been recognized as the material that binds aggregates together to provide the required mechanical properties when used in structural applications [3]. More than 4 billion metric tons of Portland cement (PC) are generated through industrial processes, releasing double carbon emissions into the atmosphere. It is why Ahmad et al. [4] stated that cement is recognized as one of the key contributors to global warming. Therefore, its reduction is always important for research in concrete so that the production can become more sustainable for the environment. Chong et al. [5] and Yurt [6] found that processes involved in cement production significantly rely on using energy to pulverize the materials together and get the required consistency of cement to make concrete. When large

* Corresponding author.
E-mail address: naraindas04@gmail.com (N. Bheel).

https://doi.org/10.1016/j.istruc.2024.106160
Received 18 May 2023; Received in revised form 26 February 2024; Accepted 3 March 2024
Available online 11 March 2024

quantities of cement are used because of the increasing demand for construction from all over the world, it directly influences the environment. This makes it important for the research to continue investigating the new materials called Supplementary Cementitious Materials (SCM) [7].

Over the last several decades, there has been significant study going on to develop concrete in which cement consumption can be minimized, which will directly impact reducing global warming and the cost of concrete production. However, DeRousseau et al. [8] and Elkady et al. [9] documented that, from a natural environment perspective, it is evident that other materials are not abundant or don't have the required learning properties that are 100% similar to cement. This is important from the perspective of maintaining the industrial production of cement, which is not going to end in the future either. Existing study on the producing concrete with other materials always relies on replacing cement with supplementary materials while maintaining the mechanical properties required for structural applications. The goal always remains to identify the optimal quantity of supplementary cementitious materials (SCM) that could be utilized in concrete to positively impact the mechanical characteristics and reduce the negative influence that easily happens on concrete by reducing the cement quality. Liang et al. [10] found that various materials are identified from existing research that is found to be similar to cement from the perspective of their pozzolanic properties. Ground-Granulated Blast Furnace Slag (GGBFS) is an effective material produced in blast furnaces. As it is a waste product from industrial processes, it negatively influences the environment. It has a high content of silicate and aluminosilicate, which are important cement components and provide binding characteristics. Rid et al. [11] stated that it is combined with ordinary Portland cement and is always known as SCM. It has highly durable characteristics that enhance the mechanical characteristics of concrete and make it more effective for structural applications. According to Karimipour et al. [12] and Zhang et al., [13] on average, the GGBFS can be added to concrete by replacing around 20% of cement. The percentage is quite important to reduce the cost of concrete production while also getting comparable mechanical characteristics without any traces of GGBFS.

Integrating GGBFS into concrete provides notable advantages in terms of corrosion resistance in the presence of reinforcement. GGBFS enhances the microstructure of concrete, reducing permeability while providing a protective barrier against the infiltration of chloride ions, a prevalent factor leading to corrosion in reinforced infrastructures [14,15]. The alkaline conditions generated by GGBFS facilitate the coating of reinforcement steel, providing further protection against corrosion. Moreover, the decrease in the heat generated during the chemical reaction of hydration reduces the probability of thermal cracking, which may create pores for corrosive substances to penetrate. GGBFS-enriched concrete is a strong option for preventing corrosion due to its higher chemical and sulphate resistance, as well as its long-term durability [16–19]. In addition to its technical advantages, the usage of GGBFS is in alignment with sustainability objectives since it is a byproduct of the steel sector. Furthermore, its implementation might result in economic gains through decreased expenses associated with long-term maintenance. In summary, GGBFS proves to be a versatile option for improving the ability of reinforced concrete buildings to resist corrosion. Introducing GGBFS into concrete often results in either a beneficial or negligible effect on creep and shrinkage. The smaller particle size and pozzolanic properties of GGBFS improve the arrangement of constituent part, leading to a reduction in the quantity of water needed and an enhancement in the convenience of handling. As a result, it contributes to a reduction in drying shrinkage and long-term deformation [20,21]. Concurrently, GGBFS has a beneficial impact on reducing Alkali-Silica Reaction (ASR) by decreasing the alkalinity of the concrete's pore solution, thereby reducing the probability of expansive gel formation and the resulting cracking [22]. Although the results may differ depending on constraints such as slag characteristics and mixture design, the general pattern indicates that GGBFS is beneficial for enhancing the concrete stability and addressing issues related to ASR.

The concrete binding properties has increasingly emphasized the use of nanomaterials because of their notable characteristics, such as their large specific surface area, enhanced reaction rate, and lowest required amount [23]. Therefore, nano-silica (NS) used as nanoparticle for this research. It is also found to be ingredient that can substitute for PC in concrete, and it has a high content of quarts, commonly known as silica dust. The high characteristics are present in NS because of the large quantities of silicon dioxide; sometimes, its percentage can reach above 99%. Nath et al. also shown that NS also has a pore-filling effect because of its small particle size [24]. The material can easily be utilized to fill the nano-pores present between the concrete aggregate, which ultimately enhances the strength characteristics because of the concrete's formation. It also has pozzolanic characteristics, which make it important to be used as SCM in concrete. It has been found that the amorphous and spherical characteristics of each particle of NS contribute to setting up the hardened concrete that are highly comparable to normal concrete [25,26]. Gan et al., [27] stated that its optimized quantity of addition in concrete is around 4%. It is because the material has a high quality of silicon dioxide, and if its percentage is increased, as in SCM in concrete, then it also shows a negative effect. Esfahani et al. [28] found that the interaction between the different materials ultimately impacts the hardened concrete, which needs to be known.

Furthermore, the researcher should explore the influence of nano-silica on creep and shrinkage appearances of GGBFS concrete, which are vital aspects that affect its overall durability. While there may be little study on this particular combination, current literature suggests that integrating nano-silica in concrete mixes, especially those that include SCM such as GGBFS, has the potential to significantly enhance durability qualities. The pozzolanic properties of NS, together with its capacity to fill microscopic spaces, have the potential to decrease water permeability and enhance strength. This might have an impact on long-term creep and shrinkage behavior. Nevertheless, in order to develop conclusive findings, it is essential to carry out empirical investigations and data-based analyses to clarify the precise impacts of NS on creep and shrinkage appearances of GGBFS concrete. This research will provide useful insights for enhancing its durability performance.

Limited research is available that focuses on combining both NS and GGBFS in cement concrete. Awolusi et al. [29] and Zhang et al. [30] stated that it did not provide valuable characteristics that could be utilized to determine the durability of high-strength concrete (HSC). This makes it important to conduct a new study that should focus on identifying the effect of NS on the mechanical and durability properties of HSC involving GGBFS. Further, it is identified that there are no implications of using Response Surface Methodology (RSM) from existing literature, from which the validator models can be obtained to predict the quantity of SCMs to be utilized in HSC to get the required mechanical and durability properties.

Therefore, this study aims to investigate the mechanical and durability characteristics of high-strength concrete involving a variable percentage of NS as nanomaterial and GGBFS as PC substitutions. Besides, the sustainability of modified HSC is determined in terms of the Embodied Carbon and Eco-Strength Efficiency. Moreover, the purpose of this investigation is to apply the RSM to findings from the mechanical and durability properties of HSC so that fully optimized models can be obtained based on the observed relationship between the mechanical characteristics and the quantity of SCMs. The implications of this study are linked with using RSM for modelling purposes and providing a proper understanding from a research perspective that can lead to the sustainable development of concrete involving NS and GGBFS.

2. Materials and methods

2.1. Materials

To make HSC, it was important to use the high-quality materials

Table 1
Chemical Composition of GGBFS and OPC.

Materials	Oxides (%)							Physical Property
	SiO_2	Al_2O_3	Fe_2O_3	CaO	Na_2O	SO_3	LOI	Specific Gravity
GGBFS	37.22	10.37	1.23	35.66	0.23	0.34	0.82	2.25
PC	20.78	5.11	3.17	60.22	0.18	2.86	2.45	3.13

Table 2
Specific characteristics of Aggregates.

Property	FA	CA
Bulk density (kg/m^3)	1858	1596
Fineness Modulus	2.21	-
SG	2.66	2.69
Absorption (%)	1.52	1.14

complying with standard specifications ASTM C33 [31]. Therefore, Portland Cement (PC) was found from local market having density of 1440 kg/m^3, ignition loss of 2.45% and fineness of 3.33%. However, the ground granulated blast furnace slag (GGBFS) was utilized as binding material and it was obtained from local industrial resources. After collecting GGBFS, it was passed through 75 μm to remove the bulky particles and then it was served as cement replacement material for PC in the production of HSC. Moreover, the Nano-silica (NS) was attained from local industrial resources and it was used as nano-material by PC weight in the production of HSC. The chemical composition of PC, and GGBFS are summarized in Table 1. In addition, the coarse aggregate (CA) of 20 mm size was obtained from the local sources having a specific gravity (SG) of 2.69. In addition, the sand was obtained with particle size less than 4.75 mm from local river sand resources and it was used as fine aggregates (FA) in HSC. Table 2 provides the specific characteristics of both FA and CA. Furthermore, water was used from the local drinking source having standard physical properties.

2.2. Mixture proportions

The mix design is based on the development of different mix ratios by which the comparative evaluation can be carried between standard high strength concrete and concrete modified with varying percentages of GGBFS and NS. One control mix and 16 modified mix ratios were developed. The GGBFS is used as SCM in high strength concrete by replacing cement from 5–20% with an 5% increment. NS is used as nano material by considering the weight of cement at 1%, 2%, 3% and 4% as shown in Table 3. The investigational runs were considered for each of the developed ratio to find out the mechanical and durability characteristics of HSC. Moreover, PC, FA, CA were added after evaluation of their primary material quality parameters. Water cement ratio was maintained at 0.35 in high strength concrete. CA, FA and Water was kept constant throughout the mixes. The flow chart of this research work as revealed in Diagram 1.

2.3. Mixing and testing

2.3.1. Mixing

Mixing of concrete was done according to BS 1881–125 [32]. Two minutes of mixing time was allocated to dry aggregates (FA and CA). GGBFS, NS and PC were added then and mixed for more 2 min. Water was added at the end and final concrete was prepared by more two minutes of mixing.

2.3.2. Testing procedure

2.3.2.1. Slump test. It was utilized to determine the workability of HSC blended with NS as nanomaterials along with GGBFS as cementitious materials by obeying BS EN 12350–2 [33]. All samples were tested by using slump cone apparatus [34–36].

2.3.2.2. Mechanical characteristics. The compressive strength test was conducted on three samples involved against each mix ratio and casted in size of 100 mm × 100 mm x 100 mm cubes. Besides, compressive testing was performed at 7, 28 and 90 days on standard compressive strength test machine at loading rate of 0.50 KN/s by monitoring BS EN 12390–3 [37] and many researchers were tested by using same procedure [38–41]. Similarly, the splitting tensile strength was carried out by observing BS EN 12390–6 [42]. Three cylindrical samples (200 mm × 100 mm) were casted for each mix ratio and then tested by utilizing the splitting tensile strength assembly in compression testing machine at the loading rate of 0.50 KN/s after 28 days only [43–46]. Moreover, the BS EN 12390–5 [47] was followed to carry out the flexural strength test of HSC. Three beam samples (500 mm × 100 mm x 100 mm) were made for each mix ratios and by using the flexural test

Table 3
Mix design of high strength concrete.

Mix ID	Ingredients (%)			Quantity of components required to generate 1 m^3 of HSC					
	PC	**GGBFS**	**NS**	**PC**	**GGBFS**	**NS**	**FA**	**CA**	**Water**
C	100	0	0	585	0	0	948	1520	210
GGBFS5NS1	95	5	1	555.75	29.25	5.85	948	1520	210
GGBFS5NS2	95	5	2	555.75	29.25	11.70	948	1520	210
GGBFS5NS3	95	5	3	555.75	29.25	17.55	948	1520	210
GGBFS5NS4	95	5	4	555.75	29.25	23.40	948	1520	210
GGBFS10NS1	90	10	1	526.50	58.50	5.85	948	1520	210
GGBFS10NS2	90	10	2	526.50	58.50	11.70	948	1520	210
GGBFS10NS3	90	10	3	526.50	58.50	17.55	948	1520	210
GGBFS10NS4	90	10	4	526.50	58.50	23.40	948	1520	210
GGBFS15NS1	85	15	1	497.25	87.75	5.85	948	1520	210
GGBFS15NS2	85	15	2	497.25	87.75	11.70	948	1520	210
GGBFS15NS3	85	15	3	497.25	87.75	17.55	948	1520	210
GGBFS15NS4	85	15	4	497.25	87.75	23.40	948	1520	210
GGBFS20NS1	80	20	1	468	117	5.85	948	1520	210
GGBFS20NS2	80	20	2	468	117	11.70	948	1520	210
GGBFS20NS3	80	20	3	468	117	17.55	948	1520	210
GGBFS20NS4	80	20	4	468	117	23.40	948	1520	210

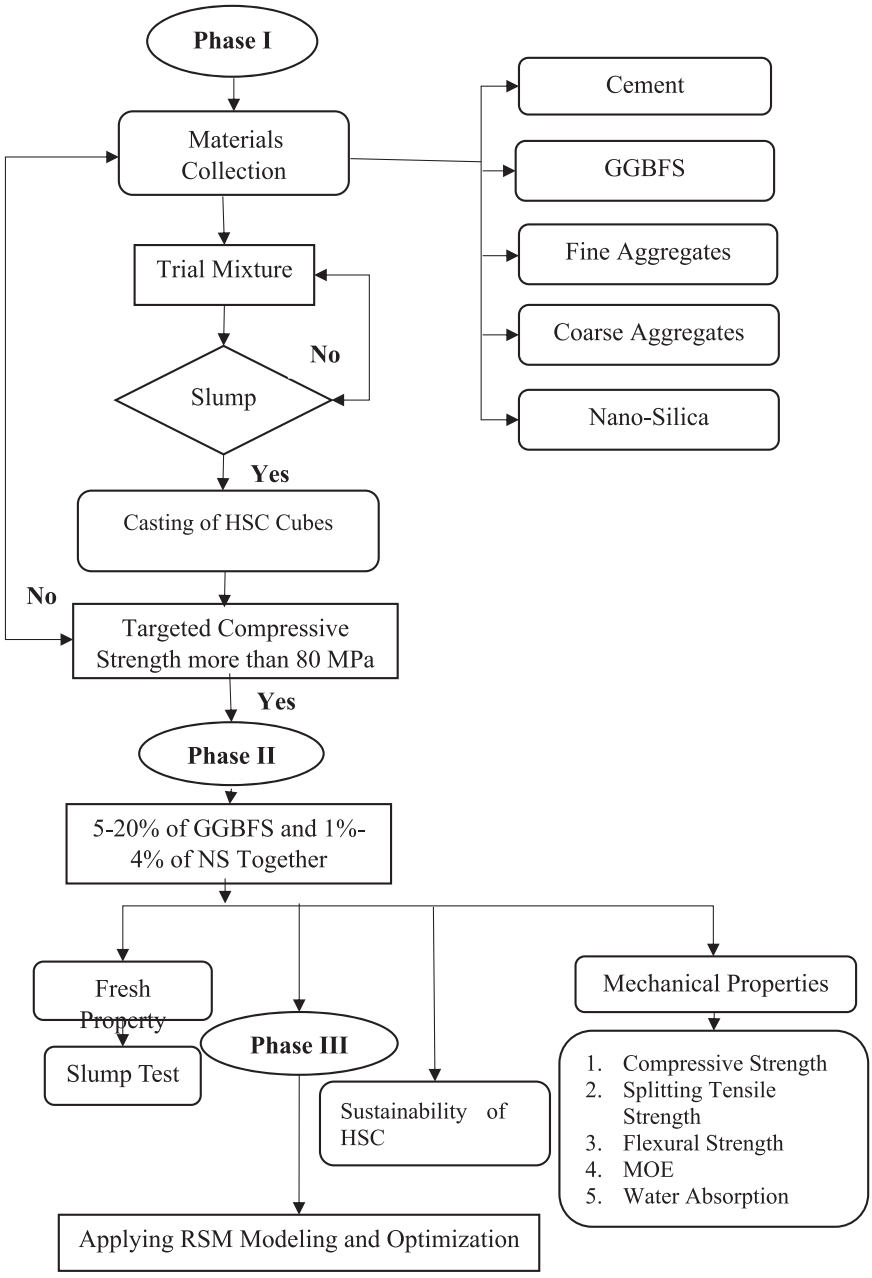

Diagram 1. Flow Chart of the Investigational Study.

assembly samples were tested on UTM at a loading rate of 0.05 kN/s after 28 days [48–50]. In addition, the Modulus of elasticity was performed on cylindrical samples (300 mm × 150 mm) of concrete blended with GGBFS as cementitious material and NS as nanomaterial after 28 days by using ASTM C469 [51]. Furthermore, the BS 1881–122 [52] was applied to record the waster absorption of all HSC samples at 28 days [53–55].

3. Results

3.1. Slump test

The workability of HSC was evaluated, and the maximum workability value was 72 mm in the case of control mix ratio C as shown in Fig. 1. It is found that as the percentage addition of GGBFS and NS is increased, it reduces the availability, and the minimum workability value was obtained in the case of sample GGBFS20NS4, which is 18. It means that with an increasing percentage of nanomaterials and SCM, workability is negatively impacted. The accumulation of NS has revealed a remarkable impact as compared to GGBFS. The small particle size resulted in a significant accumulation of material and increased the binding resistance, directly proportional to reduced workability [11, 56–58]. Even if the addition of GGBFS is kept at its maximum, it is found that the 4% addition of NS is not physical in the context of workability because it has reduced the workability to the point where it can be practically problematic to place the high-strength concrete. GGBFS has an increased silicon dioxide content, which is one of the reasons for its reduced workability, as the material does not have the same properties as cement. According to Singh [59], the workability of concrete reduced from 107 mm to 81 mm when the replacement of GGBFS was done from 0% to 50% as SCM. Similarly, according to Nath & Sarker [60], the value of slump and concrete flow decreases with increasing addition of GGBFS in concrete. The behaviour observed in this study also shown similar results indicating reduction in workability or flow of concrete as the

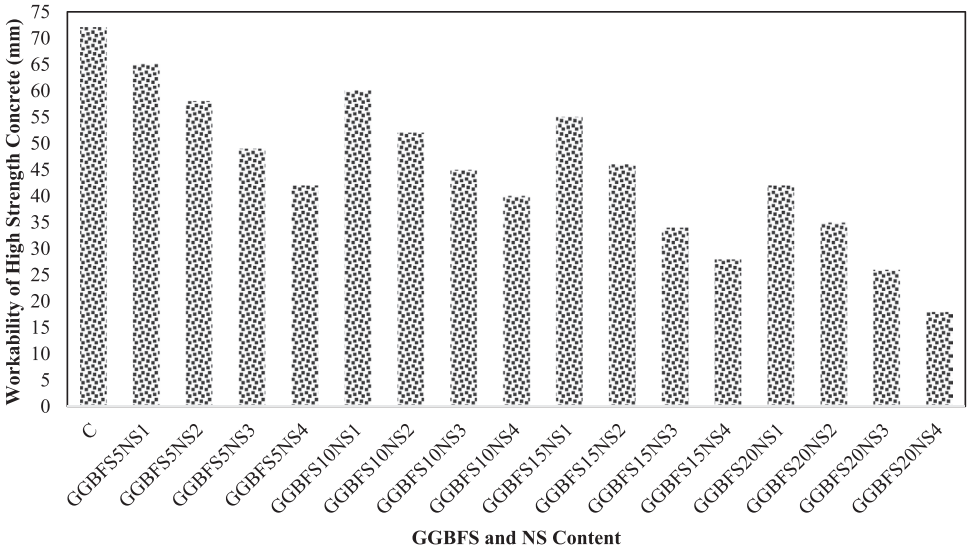

Fig. 1. Workability of high strength concrete.

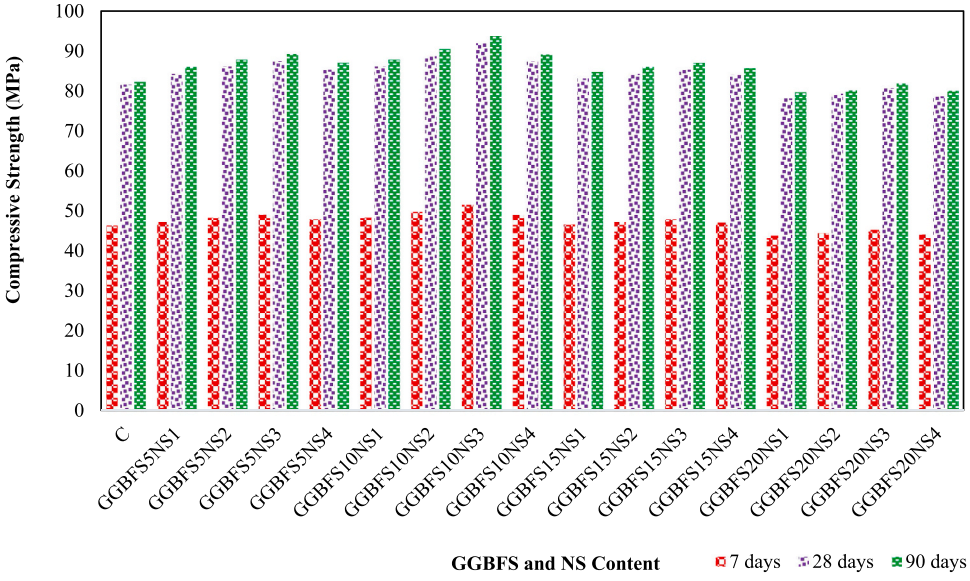

Fig. 2. Compressive strength of high strength concrete.

addition of GGBFS is increased. Adetukasi et al. [61] displayed that the workability reduces as the extent of NS rises from 0% to 10%. The similar behaviour was observed in case of Sankaranarayannan & Jagadesan [62] where the NS addition in concrete resulted in reducing the flow diameter of concrete as well its slump. The similar trend can be observed from findings of this research where the combine impact of GGBFS and NS is negative on the workability of HSC.

3.2. Compressive strength (CS)

At seven days, the high-strength control mix concrete obtained a CS of 46.2 MPa, while the maximum CS at 90 days was 82.13 MPa. The optimum 90-day CS was obtained in the case of GGBFS10NS3. It indicates that the 10% addition of GGBFS and the 3% addition of NS are feasible for HSC as revealed in Fig. 2. The other mix ratios didn't provide the high compressive strength, and it is because the increase in nanoparticles is linked with the excessive formation of chemical compounds that do not favour cement binding reactions and ultimately reduce the overall compression resistance of concrete [63,64]. The presence of high-quality silicates is the main reason behind the further reduction of CS because they reduce the concentration of calcium oxide present in overall high-strength concrete; therefore, replacing cement with more than 10% GGBFS will not provide an increase in compressive strength, which limits its use in high-strength concrete [65,66]. Similar is the case with NS because its addition to concrete concerning the weight of the cement must not increase above 3% because it has negatively impacted the concrete's compressive strength. Karri [67] concluded that the CS of cocnrete significantly rises while the GGBFS use as SCM is greater than 30%. Similar trend was found in research conducted by Kattoli et al., [68] where the CS augmented with increase in GGBFS content. However, results obtained from this study are showing increment in concrete strength but not after 10%. It is because of the fact that this research is involving GGBFS and NS together in concrete which will always has a different behaviour as compared to the past studies. According to Tawfik et al., [69], where the CS of concrete improves with addition of NS as nano material in cocnrete. The improvement however is not documented by research after 4% indicating the optimal percentage of NS to be less than 4%. Similar results are obtained by Priyadarshana et al. [70]

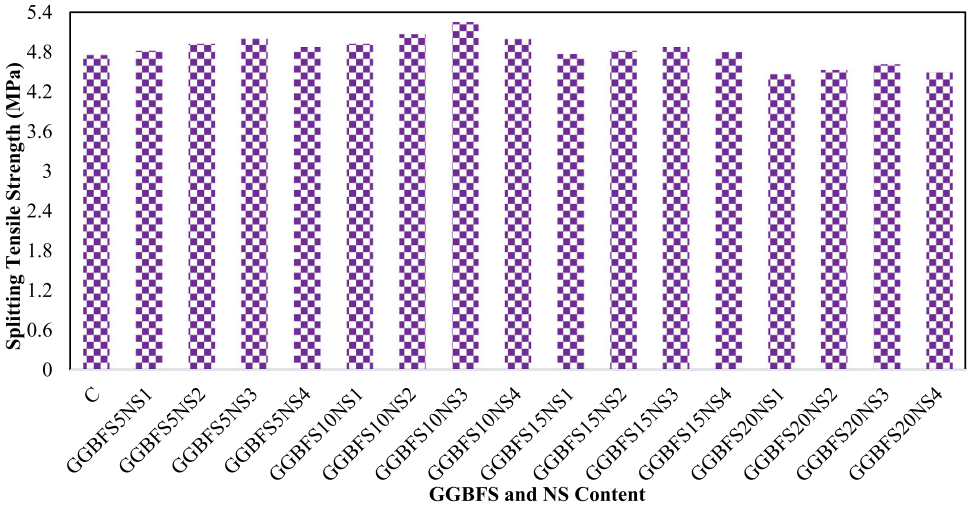

Fig. 3. Splitting Tensile Strength of high-performance concrete.

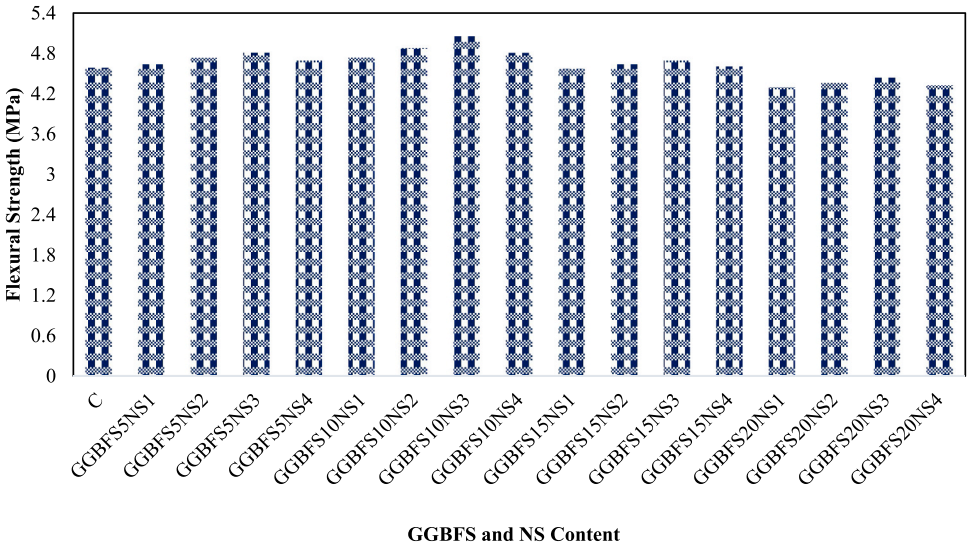

Fig. 4. Flexural strength of high-performance concrete.

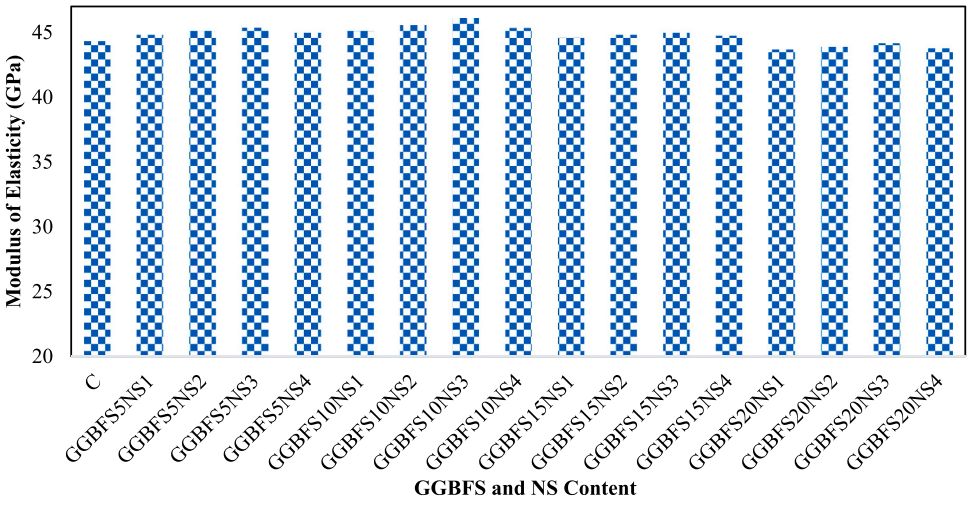

Fig. 5. Modulus of Elasticity of high strength concrete.

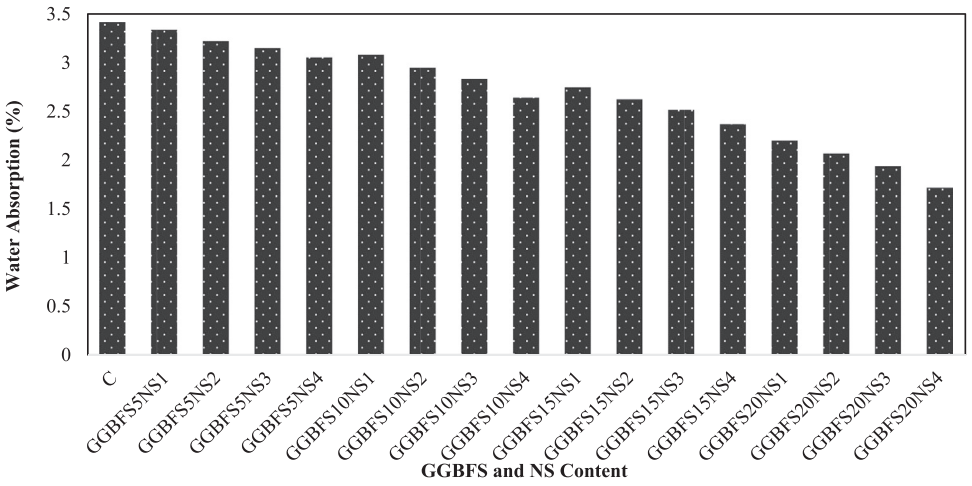

Fig. 6. Water Absorption of HSC.

Table 4
Embodied Carbon value of High Strength Concrete Components.

Components	Embodied carbon ($kgCO_2/kg$)	References
Portland cement	0.93	[97,98]
Fine aggregates	0.0139	[99]
Coarse aggregates	0.0408	[99]
GGBFS	0.07	[100]
NS	0.00084	[101,102]
Water	0	[103]

where the CS reduces as the addition of NS is increased above 2%. The observed behaviour in existing research is similar with this study but the optimal value of NS in the presence of GGBFS in concrete is found to be 3% which is unique in the context of adding nano material in the presence of GGBFS in concrete.

3.3. Splitting tensile strength (STS)

The splitting tensile test has shown positive outcomes in all samples. The control mix has a supplementing tensile strength of 4.75 MPa, while the lowest was found at GGBFS20NS1. It is found that the negative impact is happening on the STS of HSC when the addition of SCM is increased above 10%. 20% addition of GGBFS in concrete is not feasible for maximizing the STS because it has declined the strength even less than the control mix as evident from Fig. 3. However, in the case of GGBFS10NS3, it is observed that the maximum STS is obtained as compared to all other mix ratios, and it is because of the combined effect of the addition of GGBFS and NS. Silicon dioxide content increases when both additives are added in increasing quantities [71–73]. Still, the tipping point comes at 10% for GGBFS and 3% for NS when further increases in silicon dioxide content interfere with the binding characteristics of cement and ultimately reduce its mechanical properties [74,75]. However, the combined effect of both materials is positive on high-strength concrete if they are kept at the optimum level. This further strengthens the use of SCM and nanoparticles in concrete to ensure mechanical characteristics are improved. Jain et al. [76] observed that the STS of concrete can be obtained at 12.5% addition of GGBFS as SCM in concrete. Similarly, Karri [67] determined that the STS of concrete increases till the accumulation of GGBFS is kept limited to 40% but after

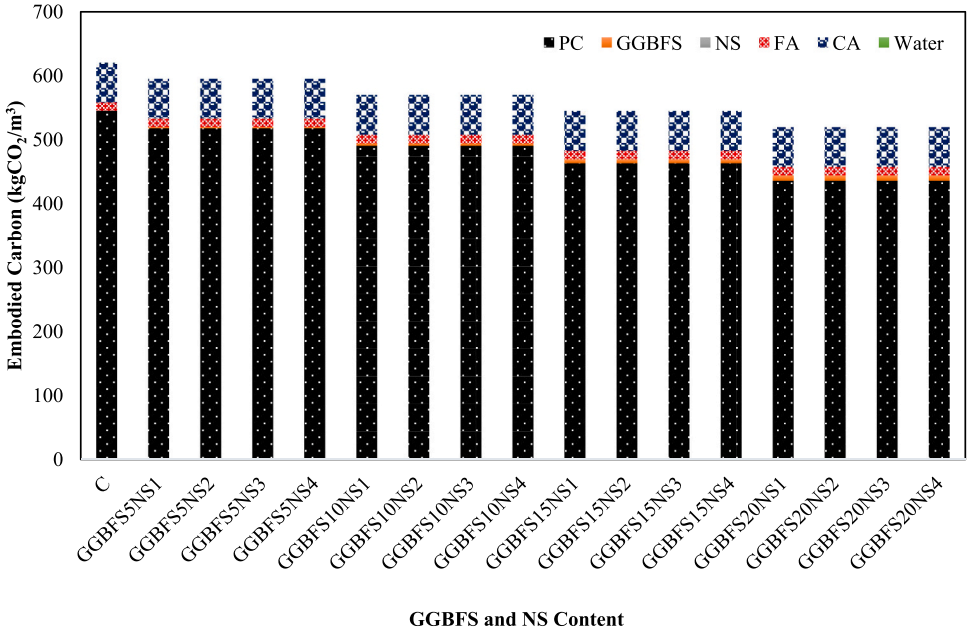

Fig. 7. Embodied carbon of high strength concrete.

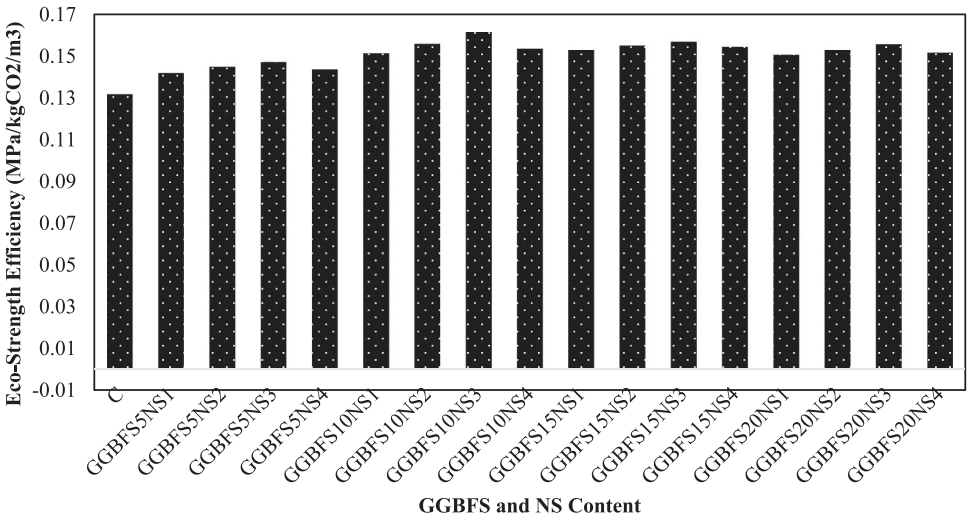

Fig. 8. Eco-Strength Efficiency of High Strength Concrete.

Table 5
RSM Runs and Responses.

Mix ID	Input Factor (%)		Responses					
	A: GGBFS	B: NS	Slump (mm)	CS (MPa)	STS (MPa)	FS (MPa)	MOE (GPa)	WA (%)
1	0	0	72	81.5	5.4	4.58	44.2733	3.4144
2	20	2	35	79.15	5.14475	4.35325	43.8436	2.068
3	20	1	42	78	5.07	4.29	43.6302	2.2
4	0	0	72	81.5	5.4	4.58	44.2733	3.4144
5	5	4	42	85.2	5.538	4.686	44.9334	3.0536
6	20	2	35	79.15	5.14475	4.35325	43.8436	2.068
7	20	4	18	78.5	5.1025	4.3175	43.7233	1.716
8	10	2	52	88.56	5.7564	4.8708	45.5165	2.948
9	10	4	40	87.28	5.6732	4.8004	45.2961	2.64
10	5	1	65	84.2	5.473	4.631	44.7569	3.3352
11	15	2	46	84.2	5.473	4.631	44.7569	2.6224
12	10	2	52	88.56	5.7564	4.8708	45.5165	2.948
13	10	4	40	87.28	5.6732	4.8004	45.2961	2.64
14	15	1	55	83	5.42	4.565	44.5433	2.7456
15	5	3	49	87.35	5.67775	4.80425	45.3082	3.1504
16	10	2	52	88.56	5.7564	4.8708	45.5165	2.948

this the negative impact was observed. The positive trend of GGBFS is similar to this study indicating increase in STS with GGBFS. But the optimal percentage of GGBFS is not same with respect to previous studies because of presence of NS and GGBFS in combine condition. Bautista-Gutierrez et al. [77] found that NS has positive impact on concrete STS when added to above 45% [77]. Similarly, Rezania et al. [78] found that STS of high strength concrete increases when NS is added upto 3%. The findings from existing research are consistent with this study because the positive trend is associated with increase in GGBFS and NS in concrete.

3.4. Flexural strength (FS)

The FS of HSC was obtained to be 4.58 MPa in the case of control mix C as evident from Fig. 4. The decrease in FS was detected after the addition of GGBFS was increased above 10%. The trend remained the same in the case of the addition of SCM to concrete in conjunction with varying percentages of NS. The bending characteristics of concrete are found to improve in the presence of NS, which is relevant to the rigid structure of concrete formed after the accumulation of nanomaterials to concrete [79–81]. The nanoparticles can establish a strong pore-filling effect, which is produced if the addition of GGBFS and NS is increased above 10% and 3%, respectively. Overall, the impact was positive for flexural strength, which is one of the deficient properties of HSC. The improvement is, however, observed in all samples during all variations of GGBFS and NS. Behaviour further indicates improvement in the mechanical credentials of concrete, which qualify both additive materials as important for manufacturing high-strength concrete. According to Karri [67], the FS of concrete initially increases with 30% addition of GGBFS in M20 concrete but decreases when GGBFS quantity is increased further. Gomathi & Sivakumar [82] found that the concrete flexural strength started to decrease after 20% addition of GGBFS. The behavior observed is in existing research is showing high percentage replacement of GGBFS in concrete as compared to this study. It is because of the fact that the GGBFS in this study is added in concrete with NS. The behavior however remained the same because the GGBFS is showing negative impact when its quantity is increased. Adetukasi et al. [61] found positice relation between the NS quantity and FS of concrete till 4%. Similar is the case with Alqamish & Al-Tamimi [79] where NS did not provided improvement in FS after 4%. Compared to this study it is clear that the FS decreases after 3% of NS, and that is similar with existing research.

3.5. Modulus of elasticity (MOE)

The MOE was conducted on HSC made cylindrical specimens blended with various content of GGBFS and NS and tested at 28 days.

Table 6
ANOVA Outcomes.

Response	Source	Sum of Squares	Df	Mean Square	F-Value	p-value > F	Significance
Slump Test	Model	2970.84	5	594.17	588.43	< 0.0001	**Yes**
	A-GGBFS	261.78	1	261.78	259.25	< 0.0001	**Yes**
	B-NS	622.30	1	622.30	616.28	< 0.0001	**Yes**
	AB	2.69	1	2.69	2.67	0.1334	**No**
	A^2	77.99	1	77.99	77.24	< 0.0001	**Yes**
	B^2	5.94	1	5.94	5.89	0.0357	**Yes**
	Residual	10.10	10	1.01			
	Lack of Fit	10.10	5	2.02			
	Pure Error	0.000	5	0.000			
	Cor Total	2980.94	15				
Compressive Strength	Model	213.70	5	42.74	45.08	< 0.0001	**Yes**
	A-GGBFS	13.03	1	13.03	13.74	0.0041	**Yes**
	B-NS	3.91	1	3.91	4.12	0.0698	**No**
	AB	1.50	1	1.50	1.58	0.2372	**No**
	A^2	44.33	1	44.33	46.75	< 0.0001	**Yes**
	B^2	5.37	1	5.37	5.66	0.0387	**Yes**
	Residual	9.48	10	0.95			
	Lack of Fit	9.48	5	1.90			
	Pure Error	0.000	5	0.000			
	Cor Total	223.18	15				
Splitting Tensile Strength	Model	0.84	5	0.17	33.06	< 0.0001	**Yes**
	A-GGBFS	0.065	1	0.065	12.70	0.0051	**Yes**
	B-NS	6.467E-003	1	6.467E-003	1.27	0.2868	**No**
	AB	9.319E-003	1	9.319E-003	1.82	0.2065	**No**
	A^2	0.18	1	0.18	34.93	0.0001	**Yes**
	B^2	0.014	1	0.014	2.73	0.1297	**No**
	Residual	0.051	10	5.107E-003			
	Lack of Fit	0.051	5	0.010			
	Pure Error	0.000	5	0.000			
	Cor Total	0.90	15				
Flexural Strength	Model	0.60	5	0.12	30.74	< 0.0001	**Yes**
	A-GGBFS	0.052	1	0.052	13.39	0.0044	**Yes**
	B-NS	5.881E-003	1	5.881E-003	1.50	0.2484	**No**
	AB	7.683E-003	1	7.683E-003	1.96	0.1915	**No**
	A^2	0.12	1	0.12	30.57	0.0003	**Yes**
	B^2	0.011	1	0.011	2.91	0.1189	**No**
	Residual	0.039	10	3.915E-003			
	Lack of Fit	0.039	5	7.830E-003			
	Pure Error	0.000	5	0.000			
	Cor Total	0.64	15				
Modulus of Elasticity	Model	6.81	5	1.36	48.35	< 0.0001	**Yes**
	A-GGBFS	0.42	1	0.42	14.89	0.0032	**Yes**
	B-NS	0.12	1	0.12	4.23	0.0668	**No**
	AB	0.046	1	0.046	1.64	0.2296	**No**
	A^2	1.41	1	1.41	50.22	< 0.0001	**Yes**
	B^2	0.16	1	0.16	5.85	0.0362	**Yes**
	Residual	0.28	10	0.028			
	Lack of Fit	0.28	5	0.056			
	Pure Error	0.000	5	0.000			
	Cor Total	7.09	15				
Water Absroption	Model	3.92	5	0.78	557.24	< 0.0001	**Yes**
	A-GGBFS	1.06	1	1.06	756.11	< 0.0001	**Yes**
	B-NS	0.11	1	0.11	76.42	< 0.0001	**Yes**
	AB	0.024	1	0.024	16.83	0.0021	**Yes**
	A^2	0.054	1	0.054	38.13	0.0001	**Yes**
	B^2	6.412E-003	1	6.412E-003	4.55	0.0586	**No**
	Residual	0.014	10	1.408E-003			
	Lack of Fit	0.014	5	2.816E-003			
	Pure Error	0.000	5	0.000			
	Cor Total	3.94	15				

However, the maximum MOE was noted at GGBFS10NS3 at 28 days. This indicates that the stiffness in the concrete is increasing, which gives rise to less elasticity or flexibility. The pore-filling effect is evident from the increase in MOE because the nanoparticles significantly impact the flexibility of high-strength concrete as shown in Fig. 5. Further, it indicates that more initial stress is required to induce failure in the material, but the mechanical failure will not be ductile compared to the control sample with a MOE of 44 MPa. However, it is also found that GGBFS20NS1 has shown the lowest MOE of 43 MPa. It indicates better ductility in concrete, but again, the other mechanical properties are reduced because the initial stress-handling capacity of concrete is reduced [83–85]. It becomes more flexible because of the increased content of silicon dioxide and the reduced binding force of cement. The behavior observed from MOE indicates a moderate negative impact on the durability of concrete when the accumulation of GGBFS and NS is increased. Still, the values are not critical as the variation happening in ductility is minor. Fikri et al. [85] found that the cocnrete MOE starts to decrease after 15% GGBFS. Yurt [6] also stated the similar behavior because particle size and cementitious properties of GGBFS are not entirely same as cement. Observed findings from this investigations are consistent with existing study showing evidence change in MOE trend. Liang et al. [10] stated that the MOE of concrete modified with NS soes

Table 7
Model Validation.

Model Validation Constraints	Slump	CS	STS	FS	MOE	WA
Std. Dev.	1.00	0.97	0.071	0.063	0.17	0.038
Mean	47.94	83.87	5.47	4.63	44.69	2.74
C.V.%	2.10	1.16	1.31	1.35	0.38	1.37
PRESS	44.51	23.48	0.12	0.099	0.70	0.058
-2 Log Likelihood	38.04	37.03	-46.55	-50.80	-19.22	-67.16
R-Squared	0.9966	0.9575	0.9429	0.9389	0.9603	0.9964
Adj R-Squared	0.9949	0.9363	0.9144	0.9084	0.9404	0.9946
Pred R-Squared	0.9851	0.8948	0.8630	0.8451	0.9010	0.9852
Adeq Precision	86.002	17.399	15.081	14.686	17.992	75.901
BIC	54.68	53.67	-29.91	-34.17	-2.59	-50.53
AICc	59.37	58.37	-25.22	-29.47	2.11	-45.83

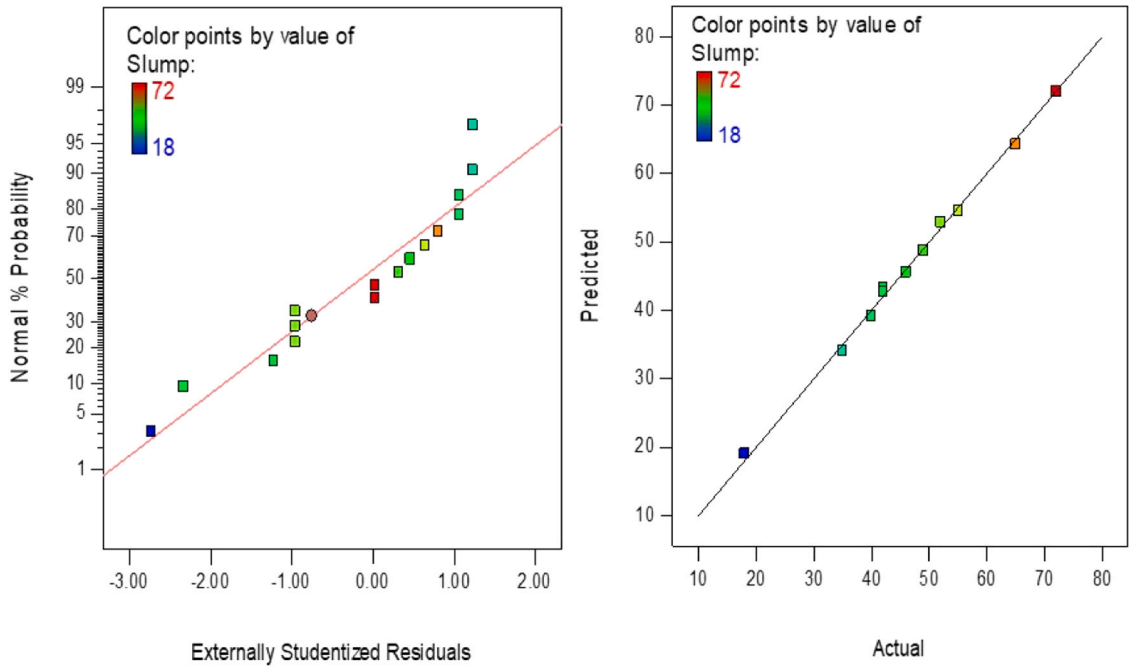

Fig. 9. Normal Plot of Residuals (Left); Actual versus Predicted Plot for Slump Test (Right).

not increase when it is increased above 4%. Karimipour et al. [12] also found the simlar behavior in cocnrete MOE indicating less feasibility of using NS above 4%. The results of this investigation align with previous studies showing that higher quantities of NS are not feasible.

3.6. *Water absorption (WA)*

It was found to be decreasing as GGBFS and NS were added. This is due to the fact that control concrete mixtures possess more internal pores, which absorb a high amount of water, while the addition of both additives in concrete decreases the pores, which results in reducing water absorption, as shown in Fig. 6. If seen from the perspective of GGBFS10NS3, the water absorption was 2.83%, indicating the high durability of concrete compared to normal concrete, which has a water absorption of 3.41%. The durability is linked with water absorption. It is evident that the nanoparticles have a strong effect on filling the pores at the nanoscale, resulting in a low probability of water absorption in the concrete matrix [86–88]. The thin coating of material combined with cement on aggregates has also affected the ability of aggregates to absorb water, resulting in a considerable decreasing in water absorption as the maximum addition of GGBFS and NS was performed in the case of GGBFS20NS4. This indicates a positive impact on durability with the addition of GGBFS and NS to the maximum, but a negative impact is observed in the case of mechanical properties. However, the findings prove the durability improvement with the addition of SCM and nano-particles. Yurt [6] found that the GGBFS addition in concrete is inversely proportional to concrete WA. The behaviour is consistent with this study where GGBFS is creating reduction of WA. Rasin et al. [89] attained that the WA was reduced with rise in NS concentration. Concrete WA changes from 8% to 4% with addition of 4% NS and this is an indication of increase in durability of concrete. Elrahman et al. [90] concluded that concrete WA sgnificantly decreases when the NS quantity is increased till 4%. The similar behaviour is observed in this research showing the improvement in durability of concrete with increasing addition of NS in high strength concrete.

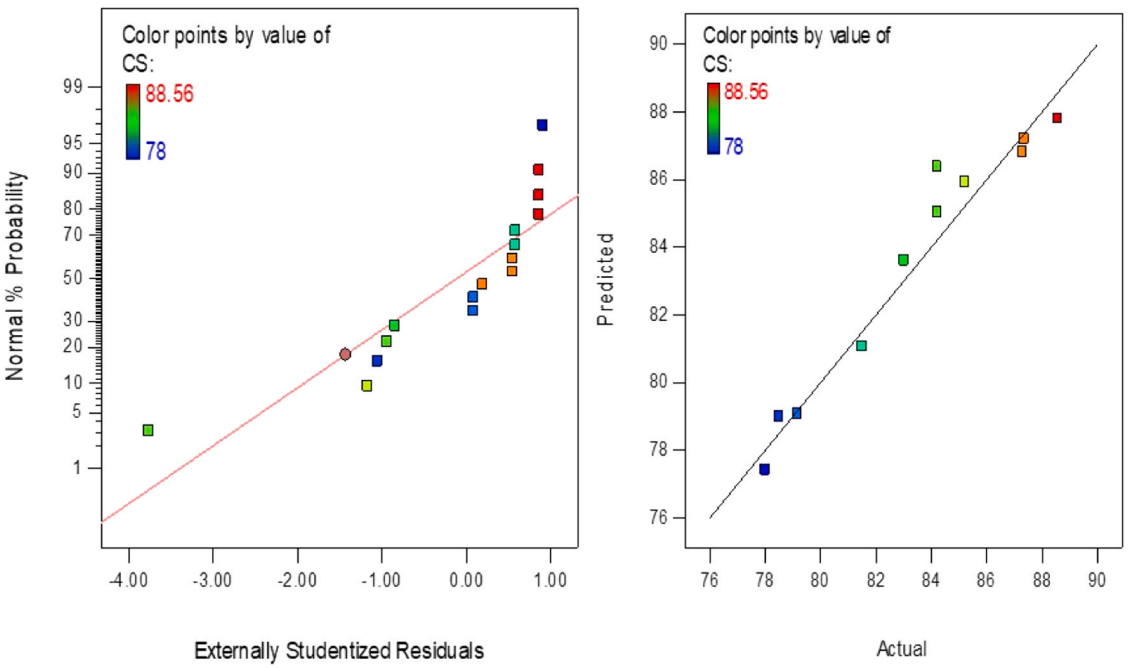

Fig. 10. Normal Plot of Residuals (Left); Actual versus Predicted Plot for CS (Right).

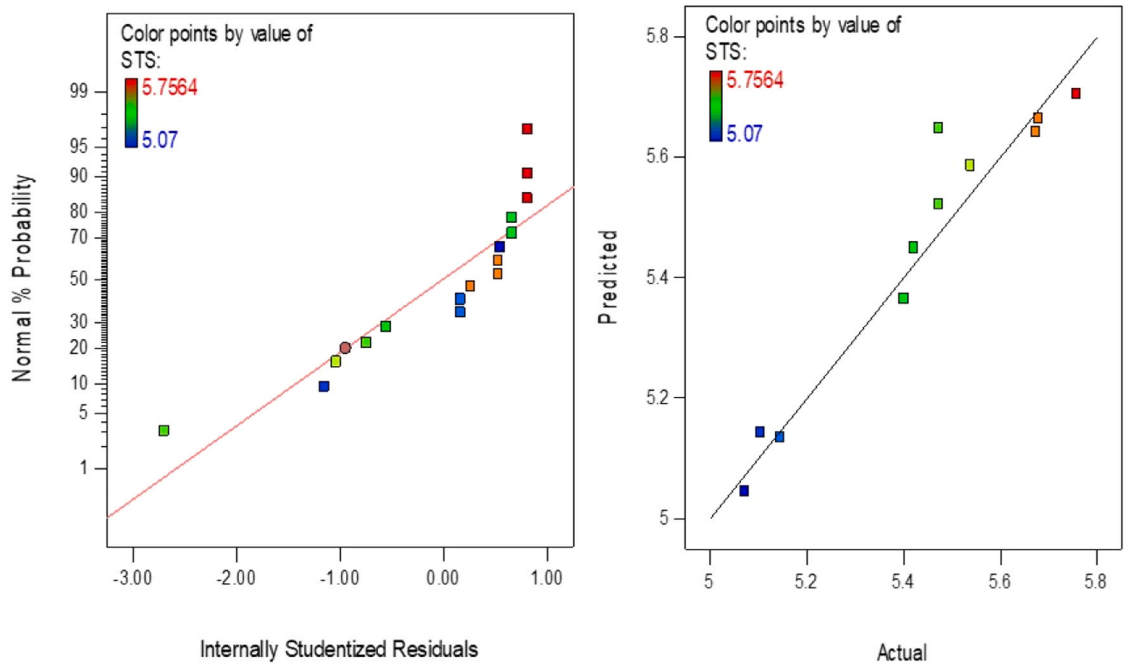

Fig. 11. Normal Plot of Residuals (Left); Actual versus Predicted Plot for STS (Right).

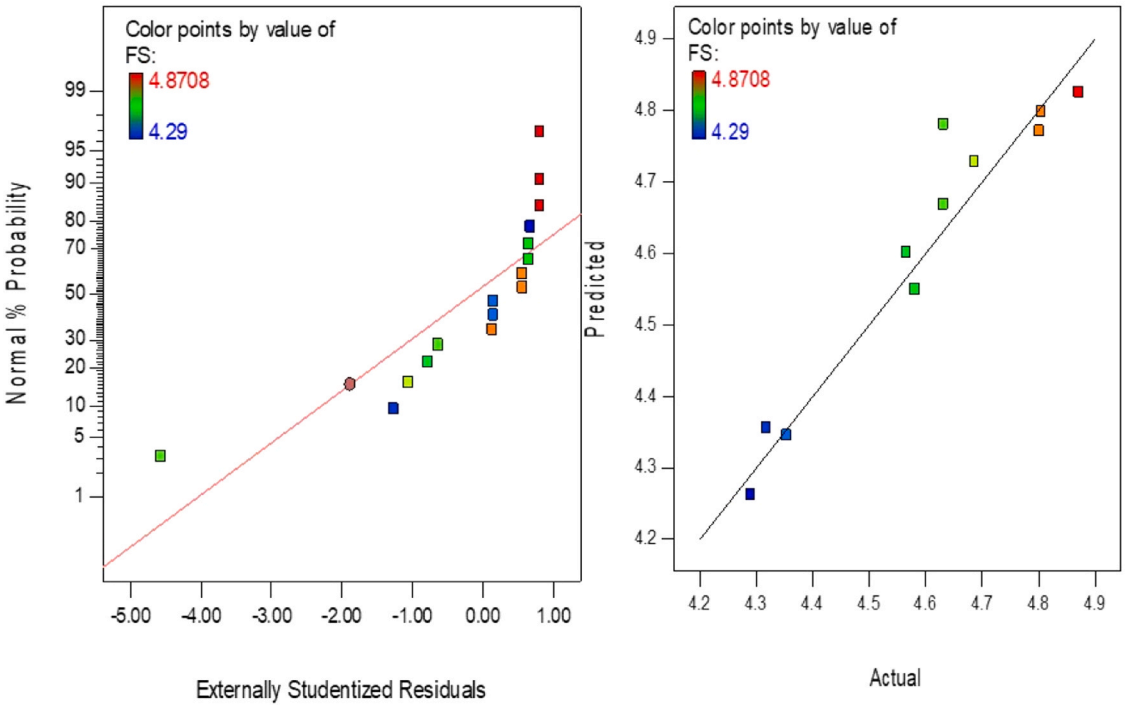

Fig. 12. Normal Plot of Residuals (Left); Actual versus Predicted Plot for FS (Right).

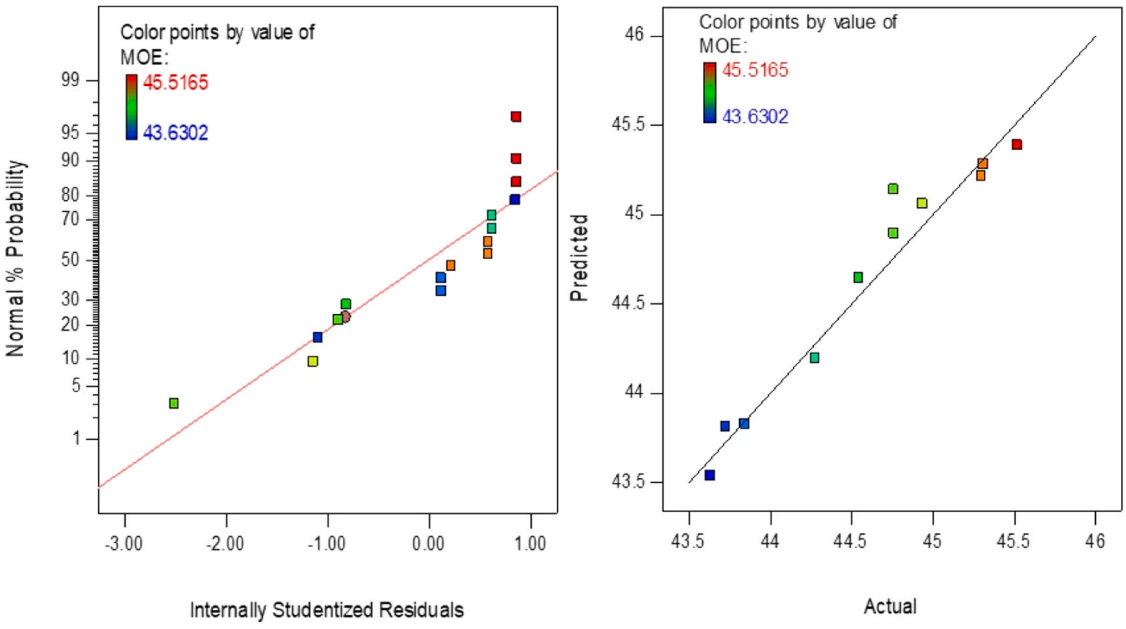

Fig. 13. Normal Plot of Residuals (Left); Actual versus Predicted Plot for MOE (Right).

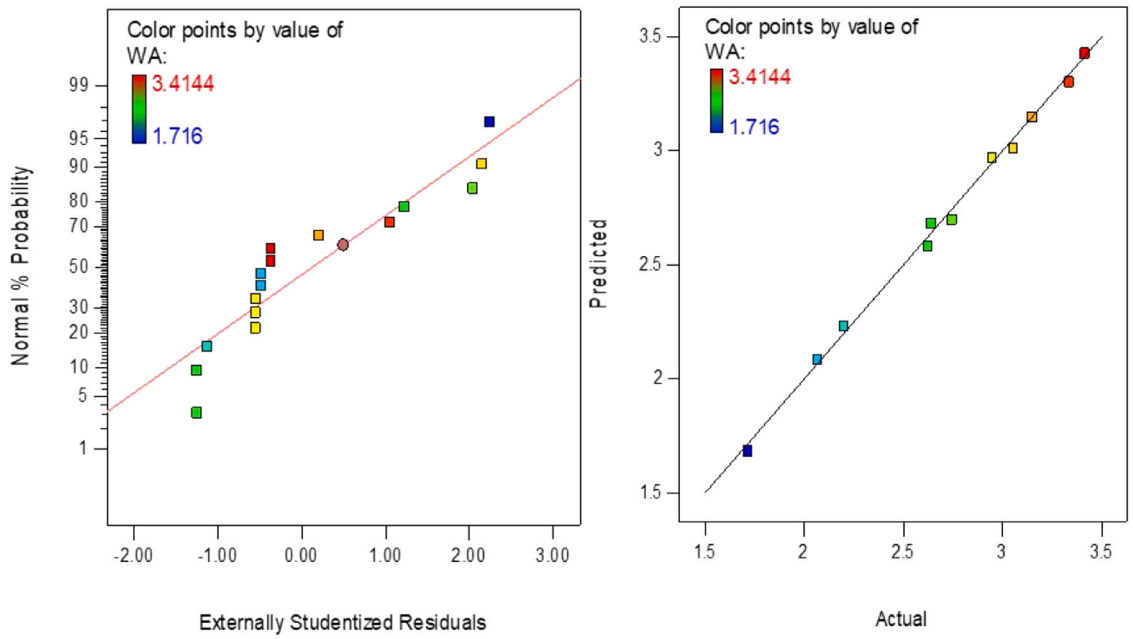

Fig. 14. Normal Plot of Residuals (Left); Actual versus Predicted Plot for WA (Right).

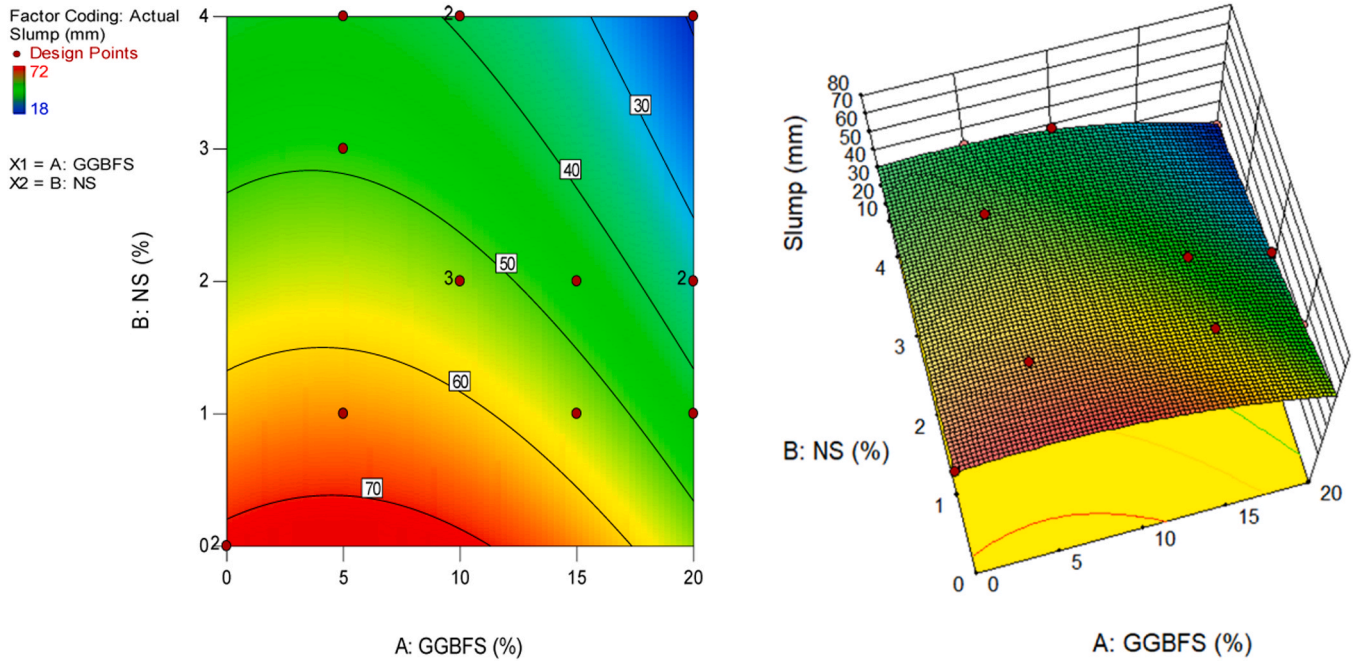

Fig. 15. Slump test of Concrete Plots – 2-D Contour Plot (Left); 3-D Response Surface Diagram (Right).

.

4. Sustainability of HSC

4.1. Embodied carbon

Every building material used in construction has some level of environmental footprint, which corresponds to the release of greenhouse gases into the atmosphere [91]. It is because every construction material goes through a variety of processes, such as extraction, transportation, manufacturing, and installation; because of the significant involvement of processes that use non-renewable energy sources, the overall procurement of materials for the building work results in greenhouse gas emissions. The embodied carbon corresponds to the greenhouse gas emissions of materials before they are practically used in construction work. It is different for every material, but when the materials are going through industrial manufacturing processes, then it is always high for every kilogram of material produced [92–94]. The calculation of embodied carbon is based on the release of carbon dioxide for every kilogram of material produced, either in industry or through all the processes involving extraction and transporting the material to the construction site. Equation 1 is used to calculate embodied carbon of material. Reduction of embodied carbon is the main priority if sustainability needs to be increased, and therefore materials with low environmental footprints are preferred for construction work [95,96]. From

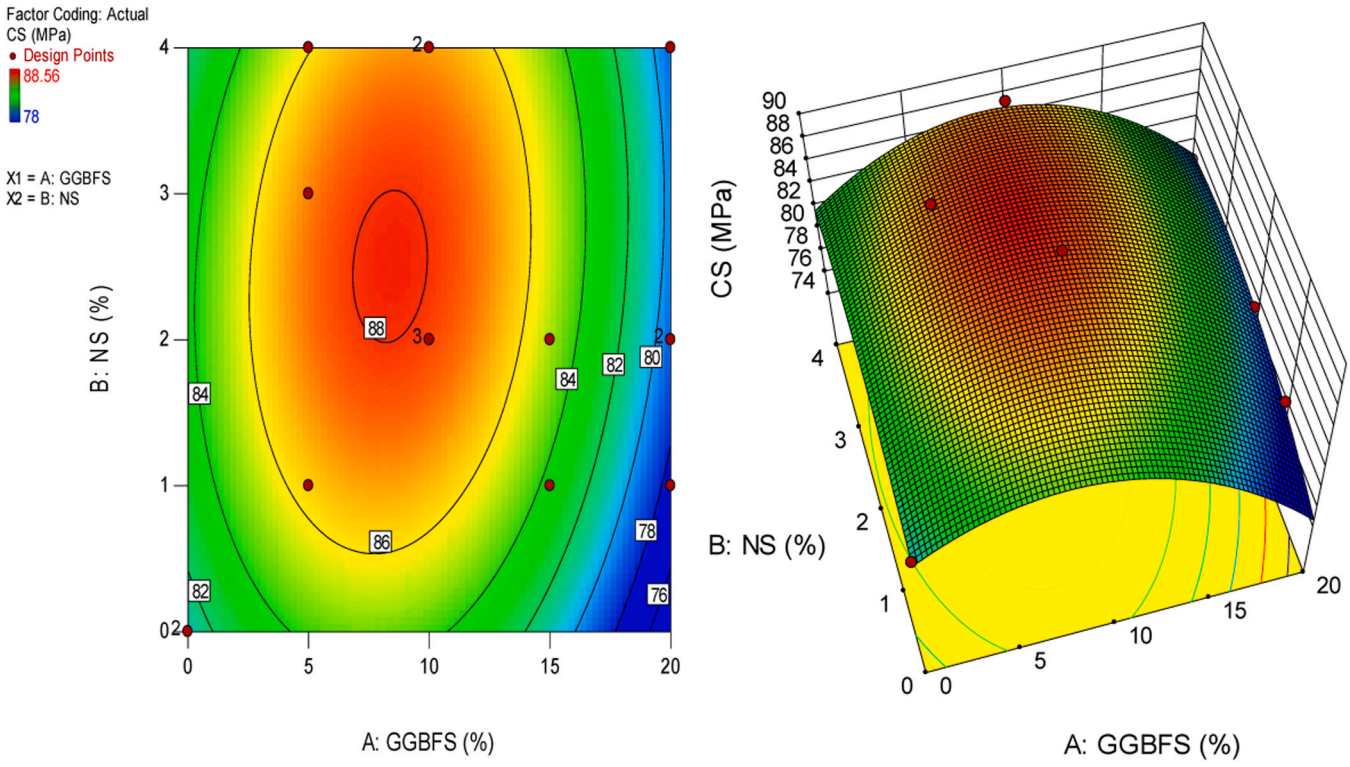

Fig. 16. Compressive Strength of Concrete Plots – 2-D Contour Plot (Left); 3-D Response Surface Diagram (Right).

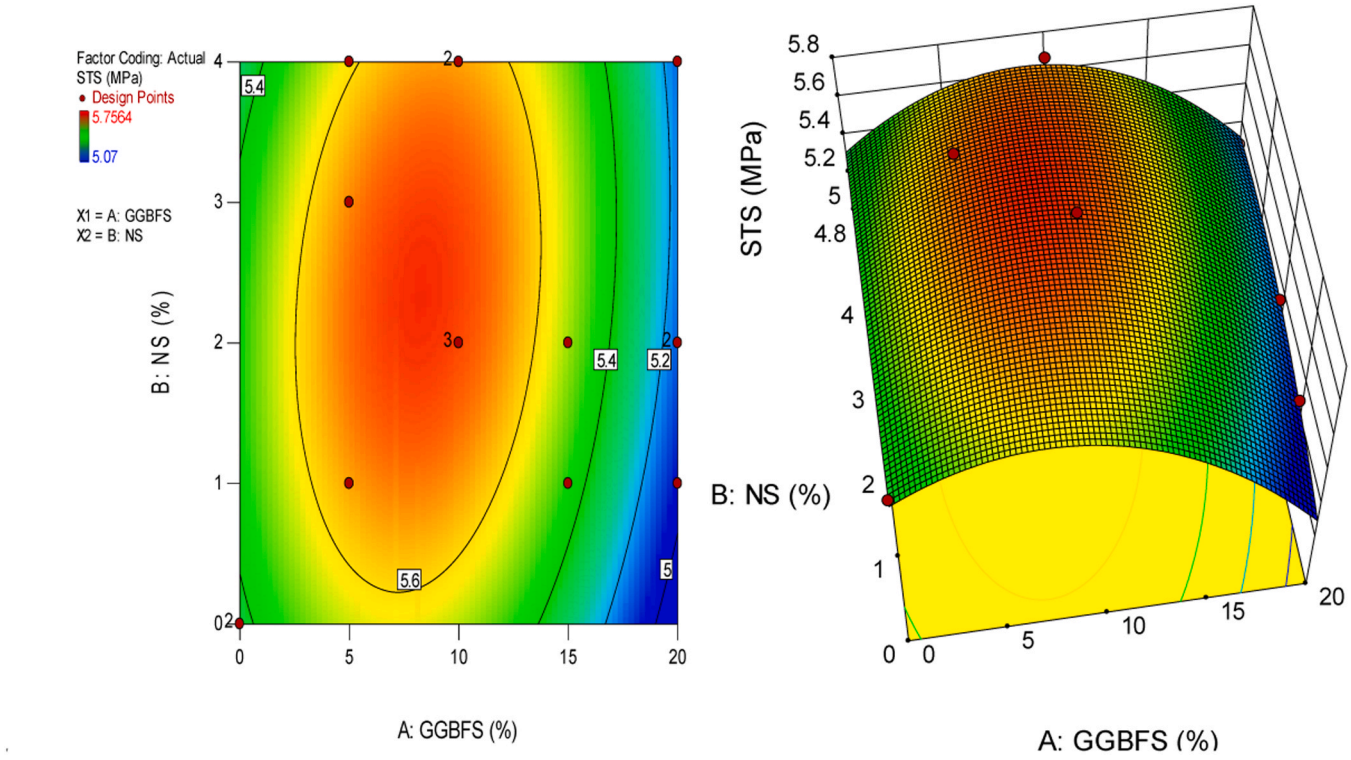

Fig. 17. Splitting Tensile Strength of Concrete Plots – 2-D Contour Plot (Left); 3-D Response Surface Diagram (Right).

Table 4, it is evident that PC has the highest embodied carbon, at 0.93 kg of carbon dioxide per kilogram. Other materials have a significantly lower carbon footprint per kilogram, which is why they are considered to be more suitable for the environment as compared to cement. From the standard values, it is clear that water has zero kilograms of carbon dioxide emissions because it is readily present in the environment, and there is no process needed to use it in construction work. However, it becomes clear that GGBFS and NS have very low embodied carbons of 0.07 and 0.00084, which is significantly less than the cement and indicates environmental sustainability if the usage of GGBFS and NS

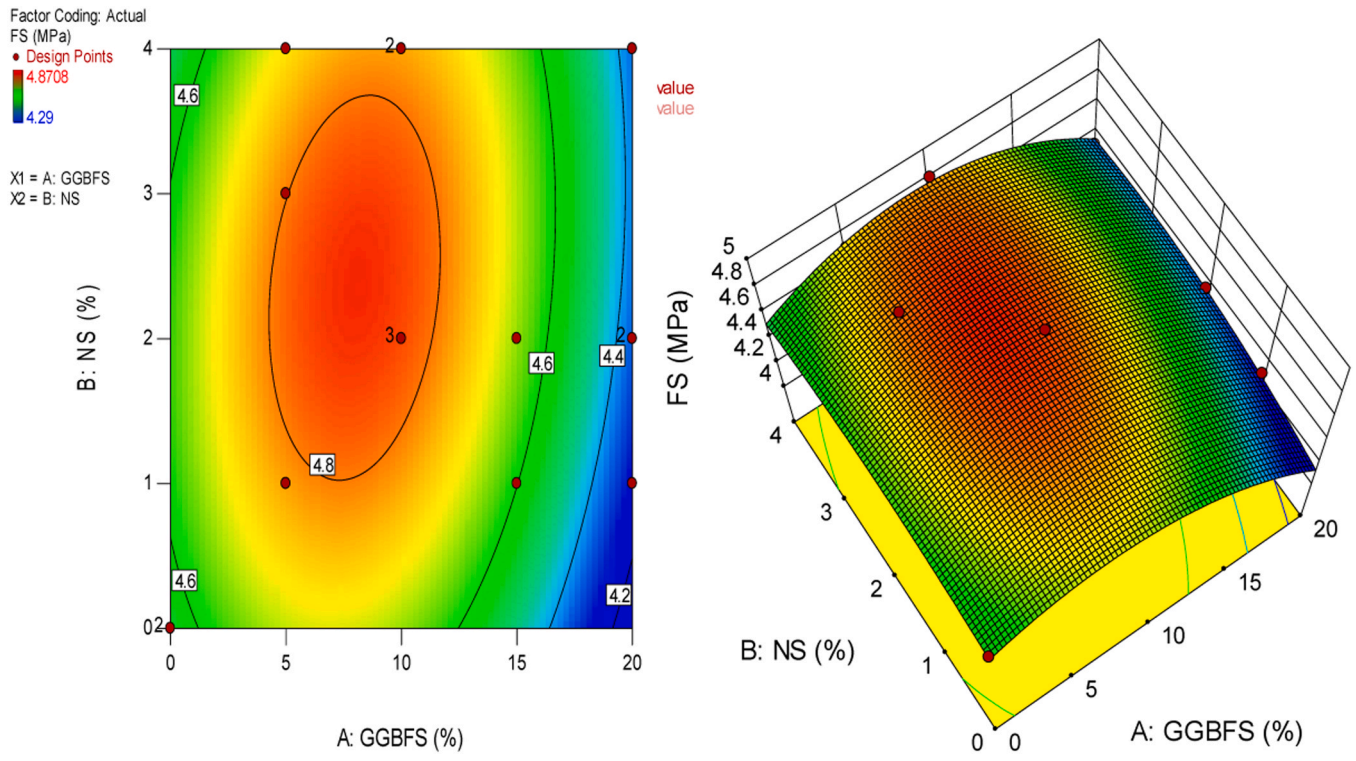

Fig. 18. Flexural Strength of Concrete Plots – 2-D Contour Plot (Left); 3-D Response Surface Diagram (Right).

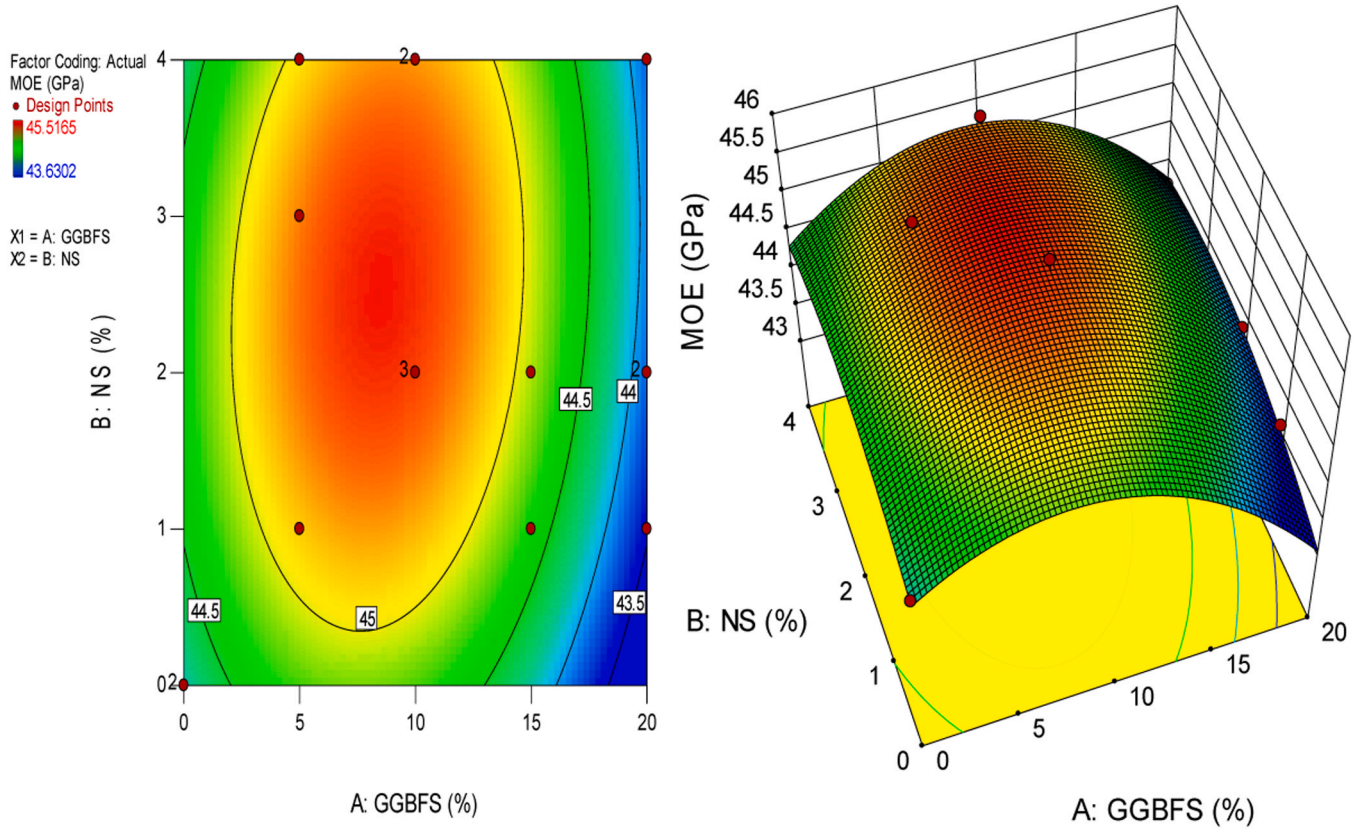

Fig. 19. MOE of Concrete Plots – 2-D Contour Plot (Left); 3-D Response Surface Diagram (Right).

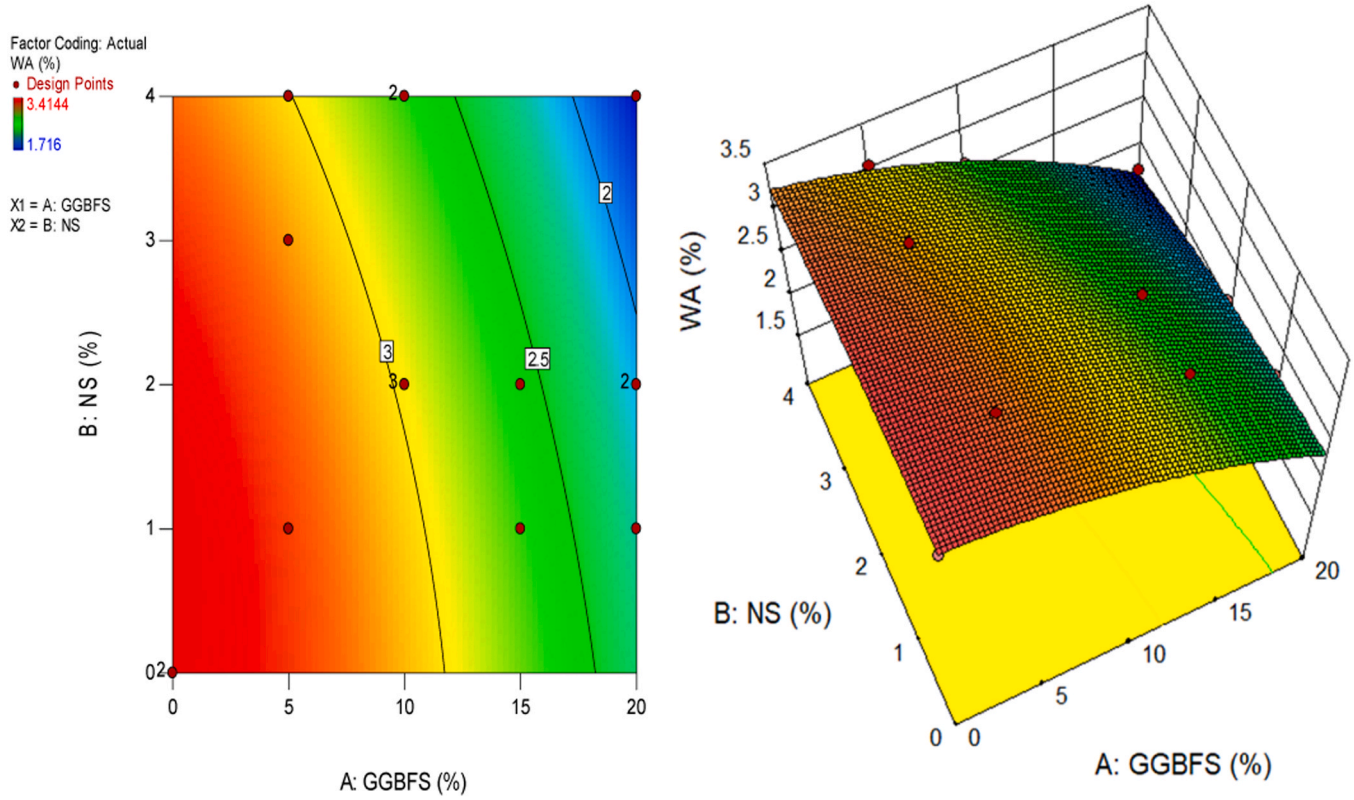

Fig. 20. Water Absorption of Concrete Plots – 2-D Contour Plot (Left); 3-D Response Surface Diagram (Right).

Table 8
Optimization goals and results.

Factors		Input Factors		Responses (Output Factors)					
		GGBFS (%)	NS (%)	Slump (mm)	CS (MPa)	STS (MPa)	FS (MPa)	MOE (GPa)	WA (%)
Value	Minimum	0	0	18	78	5.07	4.29	43.63	1.71
	Maximum	20	4	72	88.56	5.77	4.87	45.51	3.41
Goal		Range	Range	Minimize	Maximize	Maximize	Maximize	Maximize	Minimize
Optimization Results		11.34	3.54	40.18	87.11	5.65	4.78	45.26	2.65
Desirability						0.723 (72.3%)			

happens in HSC with the effective removal of cement.

$$CO_2 = \sum_{i=1}^{n} (W_i \times \quad CO_{2i-e}) \tag{1}$$

where, CO_2 is total embodied CO_2 of 1 m^3 concrete, in kg CO_2/m3.
n is total raw materials in mix,
W_i is total amount in kilogram of material.
i to produces 1 m^3 concretes.
CO_{2i-e} is equivalent CO_2 value of material i in kg CO_2/kg.

4.2. Embodied carbon of high strength concrete

The embodied carbon is significantly higher in the control sample, and it is because there is 100% cement content present in it without any additive materials that have low embodied carbon as shown in Fig. 7. The trend observed through the findings has shown that the high-strength concrete embodied carbon is reduced when the maximum percentage addition of GGBFS and NS is carried out at 20% and 4%, respectively. This is because the cement content has been reduced by 20% and is being replaced by GGBFS in high-strength concrete, which ultimately results in the introduction of embodied carbon. The positive behaviour is observed from a sustainability perspective, as both the SCM and nanoparticles have reduced the environmental footprint of high-strength concrete as indicated in case of GGBFS20NS1, GGBFS20NS2, GGBFS20NS3 and GGBFS20NS4. Similar type of trend was observed in prior research [104].

4.3. Eco-Strength Efficiency of High Strength Concrete

As the compressive strength is the main mechanical property of high-strength concrete, it can be used to calculate the eco-strength efficiency. With respect to Eq. 2, the ratio between the 28-day compressive strength of concrete and the total embodied carbon was calculated. It is an effective representation of the efficiency of concrete with respect to achieving the desirable 28-day compressive strength of high-strength concrete. This provides a valuable understanding of the most appropriate ratio that is related to the compressive strength and embodied carbon which determined the eco-strength efficiency [105]. It is indicated that GGBFS and NS additions to concrete with 10% and 3%, respectively, have resulted in achieving the eco strength of 0.16 MPa/kgCO2/m^3 in high-strength concrete as shown in Fig. 8. GGBFS10NS3 can be regarded as the most efficient mix ratio which can help to reduce environmental footprint of concrete and achieve high strength that is valuable from structural applications perspective. In case

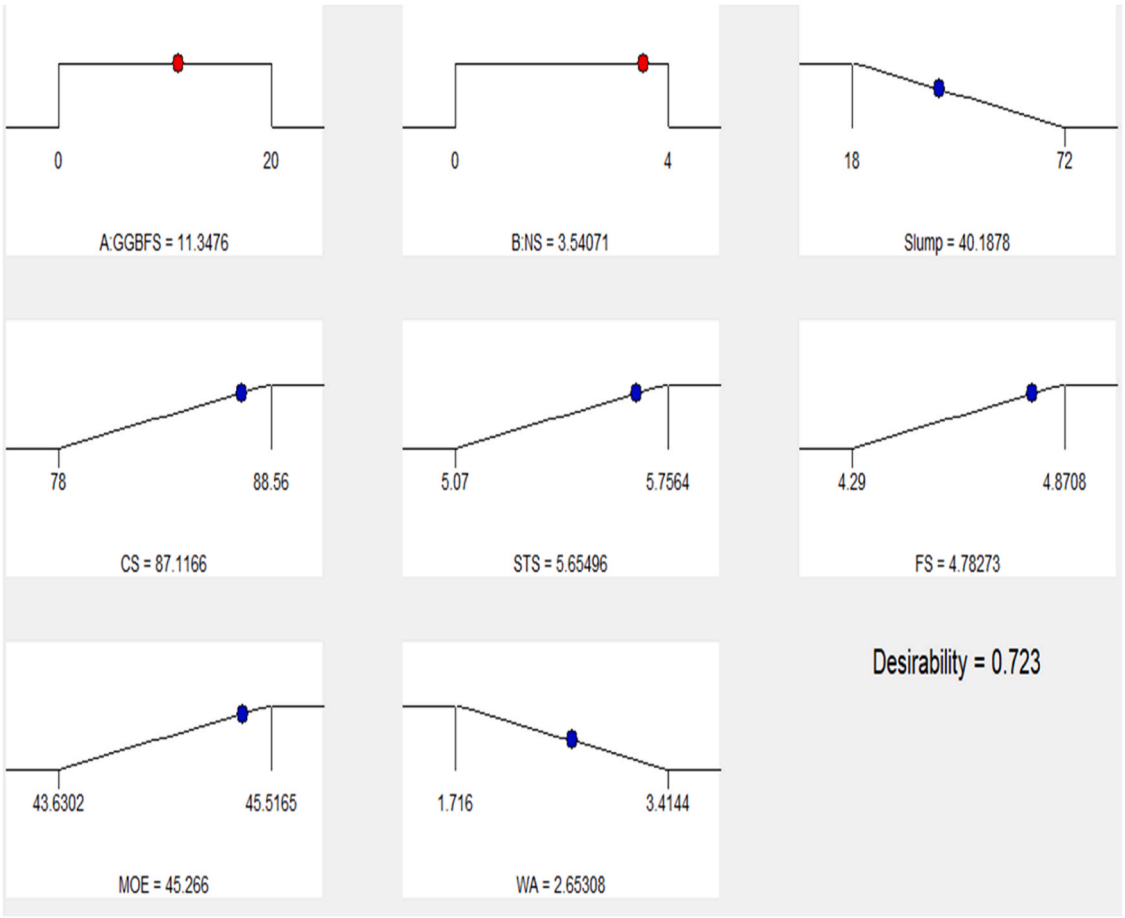

Fig. 21. Optimization solution ramp.

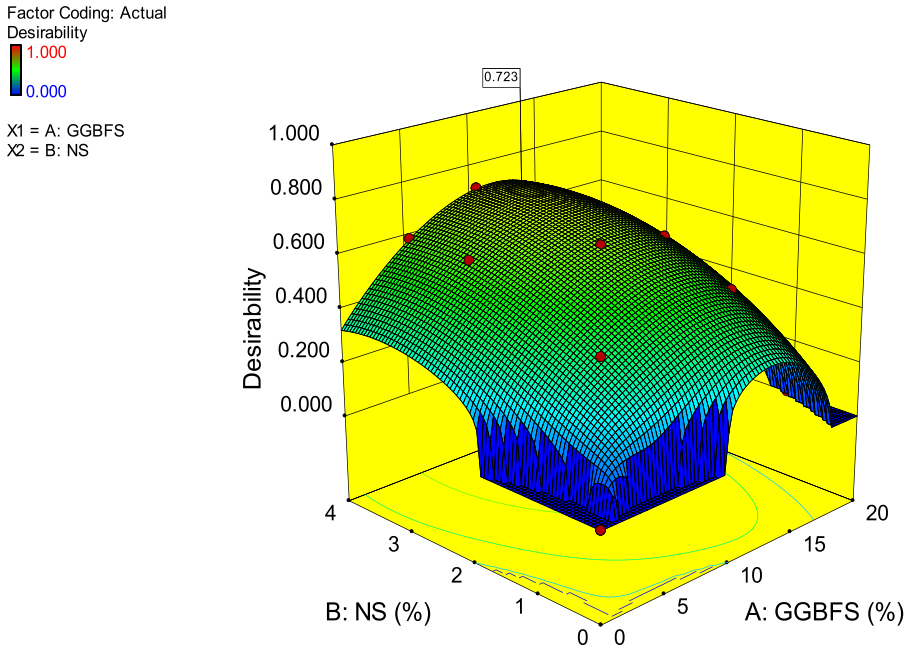

Fig. 22. Three-dimension response surface diagram for the desirability of the optimization.

Table 9
Experimental validation results of optimized value.

Response	Predicted	Experimental	Error (%)
Slump	40.18 (mm)	38.95 (mm)	3.06
CS	87.11 (MPa)	91.06 (MPa)	4.53
STS	5.65 (MPa)	5.39 (MPa)	4.60
FS	4.78 (MPa)	4.94 (MPa)	3.34
MOE	45.26 (GPa)	47.30 (GPa)	4.50
WA	2.65 (%)	2.54 (%)	4.15

of control sample C, the eco-strength efficiency is 0.13 MPa/kgCO2/m^3. Significant increase in eco-strength efficiency has happened because of reduction of cement in concrete mixes other than control sample.

$$\textbf{Eco}-\textbf{strength}\quad\textbf{efficiency}=\frac{\textbf{Average28}-\textbf{day}\quad\textbf{compressive}\quad\textbf{strength}\quad\textbf{of}\quad\textbf{concrete}}{\textbf{Total}\quad\textbf{emboided}\quad\textbf{carbon}\quad\textbf{of}\quad\textbf{conrete}} \tag{2}$$

5. RSM modelling and optimization

Response surface methodology (RSM) is a robust statistical technique used for the purpose of designing, analyzing, optimizing, and validating experimental outcomes [106–108]. It is frequently utilized in the construction sector to experimentally construct and study the effects of varying quantities of waste substitution as a renewable resource. The goal is to determine the relationship between the variables being studied and the variables that responded. The research design of the present investigation adopted the Central Composite Design (CCD) approach in the Design Expert software. This software is known for its exceptional capabilities in constructing optimal experiments, including a mixture or combination of elements, factors, and procedures. In the present investigation, the investigators utilized the design expert RSM to develop an experimental approach by providing the input variables as well as the output variables. The input variables consisted of the percentage replacement of cement with GGBFS and NS as nanomaterials, while the response factors included the slump, CS, STS, FS, MOE, and WA. Table 5 displays the factors and their accompanying outcomes for all 16 generated mixes that were mixed with NS and GGBFS as input factors. The experimental findings were applied to create prediction techniques on the basis of response surfaces.

5.1. Response surface model development and ANOVA

Based on the findings of the experiment, observational response-predictive prototypes were developed and verified. The approach has the capability to adopt either the linear or quadratic structure denoted by Equations (3) and (4), contingent upon the correlation between the input variables and their impact on the intended outcome.

$$y=\beta_0+\beta_1x_2+\beta_2x_2+\beta_nx_n+\epsilon \tag{3}$$

$$y=\beta_0+\sum_{i=1}^{k}\beta_ix_i+\sum_{i=1}^{k}\beta_{ii}x_i^2+\sum_{j=2}^{k}\sum_{i=1}^{j=1}\beta_{ij}x_ix_j+\epsilon \tag{4}$$

The modelled equations for Slump, CS, STS, FS, MOE, and WA are presented from Equations (5) to (10). It is evident from the equations that the prediction can be made based on considering A-GGBFS and B-NS quantities to predict the durability and mechanical properties of high-strength concrete. Besides, the quadratic approaches were deemed more appropriate depending on the selected sequential model sum of squares (SMSS), which exhibited a greater number of important extra terms and the approach was not subject to aliasing. The mathematical models are displayed using coded variables with the lowest, middle, and maximum values of the input factors denoted by -1, 0, and $+1$, correspondingly.

$$Slump=+52.87-10.35\times A-16.11\times B-1.21\times AB-8.51\times A^2+2.37\times B^2 \tag{5}$$

$$CS=+87.80-2.31\times A+1.28\times B+0.90\times AB-6.41\times A^2-2.2\times B^2 \tag{6}$$

$$STS=+5.71-0.16\times A+0.052\times B+0.071\times AB-0.41\times A^2-0.11\times B^2 \tag{7}$$

$$FS=+4.83-0.15\times A+0.050\times B+0.065\times AB-0.33\times A^2-0.10\times B^2 \tag{8}$$

$$MOE=+45.39-0.41\times A+0.22\times B+0.16\times AB-1.15\times A^2-0.39\times B^2 \tag{9}$$

$$WA=+2.97-0.66\times A-0.21\times B-0.11\times AB-0.22\times A^2-0.078\times B^2 \tag{10}$$

RSM models are generated based on Slump, CS, FS, STS, MOE, and WA. The Analysis of Variance (ANOVA) approach was taken to analyse the generated RSM of each durability and mechanical property. As the modelling involves two independent variables (A-GGBFS and B-NS) for each dependent variable, the ANOVA focused on identifying the p-value and the significance of each independent variable in the model [109]. Quadratic equation-based modelling is needed in such models where the combined addition of GGBFS and NS occurs. From the results of the ANOVA analysis presented in Table 6, it is evident that the model for the slump test was significant, with only AB showing insignificant results. For CS and MOE, the AB and B-NS were not significant in the model, but the overall model was significant, showing an effective relationship between variables. For STS and FS, insignificance was found for AB, B-NS, and B^2, while the whole model is significant. WA has shown insignificance only in the case of B^2.

The validation of the developed RSM for Slump, CS, STS, FS, MOE, and WA was performed by calculating the Adeq Precision values along with R-Square. From Table 7, it is evident that the modeling for each dependent variable has shown acceptable statistics. R-Square values calculated for Slump, CS, STS, FS, MOE, and WA are 0.99, 0.95, 0.94, 0.93, 0.96, and 0.99, respectively. The value for R-square is above 0.90 for every dependent variable, which means highly precise results are produced with RSM. The Adeq Precision always compares the design point predicted values with the average prediction error in the model, and it must be greater than 4. Findings show that Adeq Precision values for Slump, CS, STS, FS, MOE, and WA are 86.002, 17.399, 15.081, 14.686, 17.992, and 75.901, respectively.

Figs. 9 to 14 (left) displays the standard residual diagrams, while the Figs. 9 to 14 (right) actual vs. Predicted for slump, CS, STS, FS, MOE and WA respectively. The information has a normal distribution, as seen by the linear relationship between the number of points. The closeness of a point to the line indicates the extent to which the information follows a

normal distribution, while a greater distance signifies the reverse. The findings demonstrate that the approach is suitable for the intended purpose and may be used to calculate the best extraction variables. The predicted values of the mathematical framework are derived by applying the prediction equation, whereas the actual values are obtained via experimental runs.

The 2D contour plots and 3D RSM diagrams presented in Figs. 15 to 20 show the interaction of GGBFS and NS with Slump, CS, STS, FS, MOE, and WA. The third variable, dependent in each diagram, is kept constant, and the variation is carried out in independent variables such as GGBFS and NS. The diagrams are color-coded according to the magnitude of outputs obtained in RSM. Considering the case of the Slump test in Fig. 15, the 2D contour plot shows red color where the outputs are creating a low intense impact on the workability of high-strength concrete [110]. The combined effect can be seen when the color is transitioning to blue, indicating a negative impact on the workability of concrete. The pore-filling effect of NS and GGBFS can be effectively seen from the 3D response surface diagram, further strengthening the predictive relationship between GGBFS, NS, and Slump. Similar behavior is shown in Figs. 16 to 20, in which the variation in CS, STS, FS, MOE, and WA can be attributable to the combined effect of NS and GGBFS when added to 3% and 10% in high-strength concrete.

5.2. Optimization

The optimization of RSM is necessary to make the model more precise and further validate it to improve its prediction capability while considering the addition of GGBFS and NS. The optimization was therefore performed for all the variables involved in the model. The goals were established for the variables according to the type of mechanical and durability properties [111]. Further, the aim of the optimization is also to find out the desirability value, which ranges from 0 to 1 [112]. High desirability values are needed to have strong optimization implemented on all models. Further, it indicates that the independent variables will give positive outcomes when used to predict the Slump, CS, STS, NS, MOE, and WA. Table 8 and Fig. 21 present the optimization statistics with goals and observed desirability for the models. The goal was to minimize Slump, CS, and WA while maximizing STS, FS, and MOE. According to optimization results, the values obtained for GGBFS, NS, Slump, CS, STS, FS, MOE, and WA are 11.34, 3.54, 40.18, 87.11, 5.65, 4.78, 45.26, and 2.65 respectively. The desirability obtained from optimization is 0.723 or 72.3%. Fig. 22 presents the final 3D RSM diagram showing the desirability of an overall optimized model. Notice that the desirability lies maximum around 10% GGBFS and 3% NS which are optimized further to 11.34% GGBFS and 3.54% NS by the optimization process of RSM.

Experimental validation was also done to determine the difference between predicted and optimized RSM results and actual findings. The results obtained are presented in Table 9 whoring the predicted, experimental, and error values calculated by Equation 9. All error values obtained are less than 5%, indicating highly efficient optimized RSM for predicting Slump, CS, STS, FS, MOE, and WA.

$$Error \quad (\%) = \alpha = \left| \frac{Experimental \quad (\beta) - Predicted \quad (\gamma)}{Predicted \quad (\gamma)} \right| \times 100 \tag{9}$$

6. Conclusion

This study was conducted to determine the effect of GGBFS as SCM and NS as nanomaterial in high-strength concrete. The mechanical and durability properties were evaluated along with the sustainability. RSM was carried out to develop the prediction model for adding GGBFS and NS in high-strength concrete.

- From experimental results, slump was found to be decreasing with increasing the percentage of GGBFS and NS. The highest workability of 72 mm was found in the case of normal high-strength concrete, and the lowest 18 mm was found in the case of GGBFS20NS4. It indicates that the addition of GGBFS and NS harms the workability of high-strength concrete. CS results show that the maximum 90 days CS 93.61 MPa can be gained in the case of GGBFS10NS3. The trend remains the same for 28 days STS, FS, and MOE with maximum values of 5.24 MPa, 5.04 MPa, and 46.06 GPa, respectively. It was found that adding GGBFS and NS more than 10% and 3% respectively results in negatively affecting the CS, STS, FS, and MOE of high-strength concrete. WA was, however, found to be decreasing, with the maximum value obtained is 3.41% in the case of normal high-strength concrete and a minimum of 1.71%. For GGBFS10NS3, the WA was 2.83%, which is not minimum but effective, considering the negative impact on mechanical properties as GGBFS and NS are increased above 10% and 3%, respectively.
- The sustainability evaluation of high-strength concrete modified with GGBFS and NS found that embodied carbon decreases when GGBFS and NS quantities are increased. It is because GGBFS reduces the quantity of cement as its percentage replacement is increased. The net embodied carbon of GGBFS10NS3 was found to be 564.84 MPa/kgCO2/m^3, which is less than normal high-strength concrete with embodied carbon of 619.24 kgCO2/m^3. The eco-strength efficiency was found to be maximum for GGBFS10NS3 with a value of 0.16 kgCO2/m^3 compared to normal high-strength concrete having an eco-strength efficiency value of 0.13 MPa/kgCO2/m^3. It indicates a positive impact on sustainability by adding GGBFS and NS in concrete at 10% and 3%, respectively.
- From ANOVA, RSM results showed significance for Slump, CS, STS, FS, MOE, and WA models. From validation, the R-Square was observed to be 0.99, 0.95, 0.94, 0.93, 0.96, and 0.99 for Slump, CS, STS, FS, MOE, and WA, respectively. R-Square higher than 0.9 indicates that the variation in output variables is explained significantly by the input variables. Adeq Precision values were 86.002, 17.399, 15.081, 14.686, 17.992, and 75.901 for Slump, CS, STS, FS, MOE, and WA, respectively. All Adeq Precision values are higher than 4, showing high prediction accuracy with minimal error in all models.
- The optimization results have shown optimized output values 11.34, 3.54, 40.18, 87.11, 5.65, 4.78, 45.26, and 2.65 for GGBFS, NS, Slump, CS, STS, FS, MOE, and WA, respectively. A strong predictive capability was found in the model, with a desirability value of 72.3%. Experimental validation of the optimized model has also provided the output values with less than 5% prediction error.
- According to optimized RSM results, it becomes clear that GGBFS and NS can be used to get high-strength sustainable concrete with less cost and environmental impact. Equations presented in the study can be used to predict the Slump, CS, STS, FS, MOE, and WA with less than 5% prediction error.

Future Direction of the Study

Research is being conducted on the potential benefits of incorporating nano-silica into high-strength concrete mixed with GGBFS as a substitute for cement. This has the potential to improve many concrete qualities. Here are many possibilities for future study that may be explored:

- **Optimization of Nano-Silica Content:** Examine the most effective amount of nano-silica, when used with GGBFS, to provide the highest possible improvement in the mechanical characteristics of high-strength concrete. Utilize advanced modelling methodologies, such as artificial intelligence or machine learning algorithms, to forecast the most favorable nano-silica concentration according to the desired characteristics of the concrete.
- **Durability Studies:** Direct attention towards the extended lifespan of concrete that includes the integration of nano-silica and GGBFS.

Evaluate the level of resistance to factors like the penetration of chloride, the impact of sulphate, and the process of carbonation. Investigate the combined impact of nano-silica and GGBFS on enhancing the long-term performance of concrete.

- Application in Real Structures: Incorporate the optimized concrete mixture into real construction components. Assess the long-term performance of these structures, taking into account various factors including their ability to bear loads, resistance to cracks, and overall stability.

Contribution of Current Research

The current research focuses on studying the effects of nano-silica in high-strength concrete mixed with ground granulated blast furnace slag (GGBFS) as a substitute for cement. Researchers are using Response Surface Methodology (RSM) modelling and optimization approaches to assess the complex relationship between the amount of nano-silica in HSC and its fresh property, mechanical characteristics, and embodied carbon. The objective of this comprehensive method is to determine the optimum amount of nano-silica and GGBFS to achieve maximum performance while minimizing harm to the environment. This research is going to provide significant knowledge for creating sustainable and high-performance building materials for construction industry.

Funding

The funding for this experimental work was provided by the Deanship of Scientific Research, Taif University, Saudi Arabia.

Declaration of Competing Interest

The authors declare that they have no known competing financial interests or personal relationships that could have appeared to influence the work reported in this paper.

Acknowledgment

The researchers would like to acknowledge Deanship of Scientific Research, Taif University for funding this work.

Institutional Review Board Statement

Not Applicable.

Informed Consent Statement

Not Applicable.

References

[1] Huang H, Yuan Y, Zhang W, Zhu L. Property Assessment of High-Performance Concrete Containing Three Types of Fibers. Int J Concr Struct Mater 2021;15. https://doi.org/10.1186/s40069-021-00476-7.
[2] Wang M, Yang X, Wang W. Establishing a 3D aggregates database from X-ray CT scans of bulk concrete. Constr Build Mater 2022;315. https://doi.org/10.1016/j.conbuildmat.2021.125740.
[3] He K, Chen Y, Xie W. Test on axial compression performance of nano-silica concrete-filled angle steel reinforced GFRP tubular column. Nanotechnol Rev 2020. https://doi.org/10.1515/ntrev-2019-0047.
[4] Ahmad S, Kumar A, Kumar K. Axial performance of GGBFS concrete filled steel tubes. Structures 2020. https://doi.org/10.1016/j.istruc.2019.12.005.
[5] Chong BW, Othman R, Jaya RP, Li X, Hasan MRM, Abdullah MMAB. Meta-analysis of studies on eggshell concrete using mixed regression and response surface methodology. J King Saud Univ - Eng Sci 2021. https://doi.org/10.1016/j.jksues.2021.03.011.
[6] Yurt Ü. High performance cementless composites from alkali activated GGBFS. Constr Build Mater 2020. https://doi.org/10.1016/j.conbuildmat.2020.120222.
[7] Jin M, Ma Y, Li W, Huang J, Yan Y, Zeng H, et al. Multi-scale investigation on composition-structure of C-(A)-S-H with different Al/Si ratios under attack of decalcification action. Cem Concr Res 2023;172. https://doi.org/10.1016/j.cemconres.2023.107251.
[8] DeRousseau MA, Arehart JH, Kasprzyk JR, Srubar WV. Statistical variation in the embodied carbon of concrete mixtures. J Clean Prod 2020;275. https://doi.org/10.1016/j.jclepro.2020.123088.
[9] Elkady HM, Yasien AM, Elfeky MS, Serag ME. Assessment of mechanical strength of nano silica concrete (NSC) subjected to elevated temperatures. J Struct Fire Eng 2019. https://doi.org/10.1108/JSFE-10-2017-0041.
[10] Liang M, Li Z, He S, Chang Z, Gan Y, Schlangen E, et al. Stress evolution in restrained GGBFS concrete due to autogenous deformation: bayesian optimization of aging creep. Constr Build Mater 2022. https://doi.org/10.1016/j.conbuildmat.2022.126690.
[11] Rid ZA, Shah SNR, Memon MJ, Jhatial AA, Keerio MA, Goh WI. Evaluation of combined utilization of marble dust powder and fly ash on the properties and sustainability of high-strength concrete. Environ Sci Pollut Res 2022;29(19):28005. https://doi.org/10.1007/s11356-021-18379-1.
[12] Karimipour A, Ghalehnovi M, Edalati M, de Brito J. Properties of fibre-reinforced high-strength concrete with nano-silica and silica fume. Appl Sci 2021. https://doi.org/10.3390/app11209696.
[13] Zhang Q, Feng X, Chen X, Lu K. Mix design for recycled aggregate pervious concrete based on response surface methodology. Constr Build Mater 2020. https://doi.org/10.1016/j.conbuildmat.2020.119776.
[14] Divsholi BS, Lim TYD, Teng S. Durability Properties and Microstructure of Ground Granulated Blast Furnace Slag Cement Concrete. Int J Concr Struct Mater 2014;8:157–64. https://doi.org/10.1007/s40069-013-0063-y.
[15] Ahmad J, Kontoleon KJ, Majdi A, Naqash MT, Deifalla AF, Ben Kahla N, et al. A Comprehensive Review on the Ground Granulated Blast Furnace Slag (GGBS) in Concrete Production. Sustain 2022;14. https://doi.org/10.3390/su14148783.
[16] Mugahed A, Amin A, Chu S, Roman F, Sani H, Afonso A, et al. Long-term durability properties of geopolymer concrete: An in-depth review. Case Stud Constr Mater 2021;15.
[17] Cong P., Cheng Y. Advances in geopolymer materials: A comprehensive review. J Traffic Transp Eng (English Ed 2021;8:283–314. https://doi.org/10.1016/j.jtte.2021.03.004.
[18] Krivenko P, Rudenko I, Konstantynovskyi O, Boiko O. Prevention of steel reinforcement corrosion in alkali-activated slag cement concrete mixed with seawater. E3S Web Conf 2021;280. https://doi.org/10.1051/e3sconf/202128007004.
[19] Huo Y, Huang J, Han X, Sun H, Liu T, Zhou J, et al. Mass GGBFS Concrete Mixed with Recycled Aggregates as Alkali-Active Substances: Workability, Temperature History and Strength. Mater (Basel) 2023;16. https://doi.org/10.3390/ma16165632.
[20] Özbay E, Erdemir M, Durmuş HI. Utilization and efficiency of ground granulated blast furnace slag on concrete properties - A review. Constr Build Mater 2016;105:423–34. https://doi.org/10.1016/j.conbuildmat.2015.12.153.
[21] Qu Z, Liu Z, Si R, Zhang Y. Effect of various fly ash and ground granulated blast furnace slag content on concrete properties: experiments and modelling. Materials 2022;15. https://doi.org/10.3390/ma15093016.
[22] Choi SY, Yang EI. An experimental study on alkali silica reaction of concrete specimen using steel slag as aggregate. Appl Sci 2020;10. https://doi.org/10.3390/APP10196699.
[23] He H, ES, Wen T, Yao J, Wang X, He C, et al. Employing novel N-doped graphene quantum dots to improve chloride binding of cement. Constr Build Mater 2023;401. https://doi.org/10.1016/j.conbuildmat.2023.132944.
[24] Nath P, Sarker PK, Biswas WK. Effect of fly ash on the service life, carbon footprint and embodied energy of high strength concrete in the marine environment. Energy Build 2018. https://doi.org/10.1016/j.enbuild.2017.12.011.
[25] Piroti S, Najarchi M, Hezavehi E, Najafizadeh MM, Mirhosseini SM. The experimental assessment of the effect of polypropylene fibers on the improvement of nano-silica concrete behavior. Sci Iran 2020. https://doi.org/10.24200/sci.2018.50514.1735.
[26] Han IJ, Yuan TF, Lee JY, Yoon YS, Kim JH. Learned prediction of compressive strength of GGBFS concrete using hybrid artificial neural network models. Mater (Basel) 2019. https://doi.org/10.3390/ma12223708.
[27] Gan VJL, Cheng JCP, Lo IMC. A comprehensive approach to mitigation of embodied carbon in reinforced concrete buildings. J Clean Prod 2019. https://doi.org/10.1016/j.jclepro.2019.05.035.
[28] Rasoul Abdar Esfahani SM, Zareei SA, Madhkhan M, Ameri F, Rashidiani J, Taheri RA. Mechanical and gamma-ray shielding properties and environmental benefits of concrete incorporating GGBFS and copper slag. J Build Eng 2021. https://doi.org/10.1016/j.jobe.2020.101615.
[29] Awolusi TF, Oke OL, Akinkurolere OO, Sojobi AO. Application of response surface methodology: Predicting and optimizing the properties of concrete containing steel fibre extracted from waste tires with limestone powder as filler. Case Stud Constr Mater 2019;10. https://doi.org/10.1016/j.cscm.2018.e00212.
[30] Zhang GZ, Cho HK, Wang XY. Effect of nano-silica on the autogenous shrinkage, strength, and hydration heat of ultra-high strength concrete. Appl Sci 2020. https://doi.org/10.3390/app10155202.
[31] ASTM C33. Standard specification for concrete aggregates. Philadelphia, PA: American Society for Testing and Materials, 2002, 2002., n.d.
[32] BS 1881–125:1986. 1986. Methods for mixing and sampling fresh concrete in the laboratory. BSI, London., n.d.
[33] BS EN 12350–2, Testing Fresh Concrete, Part 2: Slump-Test, BSI, London, UK 2009.
[34] Shariq M, Prasad J, Abbas H. Creep and drying shrinkage of concrete containing GGBFS. Cem Concr Compos 2016. https://doi.org/10.1016/j.cemconcomp.2016.02.004.

[35] Afroz S, Zhang Y, Nguyen Dieu, Kim Q, Castel T. A. Effect of limestone in General Purpose cement on autogenous shrinkage of high strength GGBFS concrete and pastes. Constr Build Mater 2022. https://doi.org/10.1016/j.conbuildmat.2022.126949.

[36] Yang H, Xu X, Neumann I. Optimal finite element model with response surface methodology for concrete structures based on Terrestrial Laser Scanning technology. Compos Struct 2018. https://doi.org/10.1016/j.compstruct.2016.11.012.

[37] BS EN 12390–3, Testing hardened concrete. Compressive strength of test specimens. London, United Kingdom: British Standards Institution, 2009. n.d.

[38] Jayasinghe A, Orr J, Hawkins W, Ibell T, Boshoff WP. Comparing different strategies of minimising embodied carbon in concrete floors. J Clean Prod 2022;345. https://doi.org/10.1016/j.jclepro.2022.131177.

[39] PP Abhilash, Nayak DK, Sangoju B, Kumar R, Kumar V. Effect of nano-silica in concrete; a review. Constr Build Mater 2021. https://doi.org/10.1016/j.conbuildmat.2021.122347.

[40] Bellum RR, Muniraj K, Madduru SRC. Exploration of mechanical and durability characteristics of fly ash-GGBFS based green geopolymer concrete. SN Appl Sci 2020. https://doi.org/10.1007/s42452-020-2720-5.

[41] Sithole NT, Tsotetsi NT, Mashifana T, Sillanpää M. Alternative cleaner production of sustainable concrete from waste foundry sand and slag. J Clean Prod 2022. https://doi.org/10.1016/j.jclepro.2022.130399.

[42] British Standards Institute. BS EN 12390–6 Tensile splitting strength of test specimens. BSI Stand Publ 2009.

[43] Poorarbabi A, Ghasemi M, Azhdary Moghaddam M. Concrete compressive strength prediction using non-destructive tests through response surface methodology. Ain Shams Eng J 2020;11:939–49. https://doi.org/10.1016/j.asej.2020.02.009.

[44] Bheel N, Sohu S, Jhatial AA, Memon NA, Kumar A. Combined effect of coconut shell and sugarcane bagasse ashes on the workability, mechanical properties and embodied carbon of concrete. Environ Sci Pollut Res 2022;29:5207–23. https://doi.org/10.1007/s11356-021-16034-3.

[45] Huynh AT, Nguyen QD, Xuan QL, Magee B, Chung T, Tran KT, et al. A machine learning-assisted numerical predictor for compressive strength of geopolymer concrete based on experimental data and sensitivity analysis. Appl Sci 2020. https://doi.org/10.3390/app10217726.

[46] Adak D, Sarkar M, Mandal S. Structural performance of nano-silica modified fly-ash based geopolymer concrete. Constr Build Mater 2017. https://doi.org/10.1016/j.conbuildmat.2016.12.111.

[47] BSI. BS EN 12390–5: 2000. Testing hardened concrete. Flexural strength of test specimens. Br Stand Inst 2000.

[48] Cong X, Zhou W, Elchalakani M. Experimental study on the engineering properties of alkali-activated GGBFS/FA concrete and constitutive models for performance prediction. Constr Build Mater 2020. https://doi.org/10.1016/j.conbuildmat.2019.117977.

[49] Fahmy M, Abu El-Hassan M, Kamh G, Bashandy A. Investigation of Using Nano-silica, Silica Fume and Fly Ash in High Strength Concrete. ERJ Eng Res J 2020. https://doi.org/10.21608/erjm.2020.95144.

[50] Adamu M, Ayeni KO, Haruna SI, Ibrahim Mansour YEH, Haruna S. Durability performance of pervious concrete containing rice husk ash and calcium carbide: A response surface methodology approach. Case Stud Constr Mater 2021. https://doi.org/10.1016/j.cscm.2021.e00547.

[51] ASTM C469. Standard Test Method for Static Modulus of Elasticity and Poisson's Ratio of Concrete in Compression. ASTM Stand B 2002;04:1–5.

[52] BS 1881: Part 122: 1983; Method for Determination of Water Absorption. British Standards Institute: London, UK; Department, C.T.S British Stand: London, UK, 1983., n.d.

[53] Hawkins W, Orr J, Ibell T, Shepherd P. A design methodology to reduce the embodied carbon of concrete buildings using thin-shell floors. Eng Struct 2020. https://doi.org/10.1016/j.engstruct.2020.110195.

[54] Kathirvel P, Sreekumaran S. Sustainable development of ultra high performance concrete using geopolymer technology. J Build Eng 2021. https://doi.org/10.1016/j.jobe.2021.102267.

[55] Anumeena S.U., Karthiyaini S. An experimental investigation on the effect of nano silica in concrete. Int J Civ Eng Technol 2018.

[56] Mostafa SA, EL-Deeb MM, Farghali AA, Faried AS. Evaluation of the nano silica and nano waste materials on the corrosion protection of high strength steel embedded in ultra-high performance concrete. Sci Rep 2021. https://doi.org/10.1038/s41598-021-82322-0.

[57] Amiri H, Azadi S, Karimaei M, Sadeghi H, Farshad Dabbaghi. Multi-objective optimization of coal waste recycling in concrete using response surface methodology. J Build Eng 2022. https://doi.org/10.1016/j.jobe.2021.103472.

[58] Thilakarathna PSM, Seo S, Baduge KSK, Lee H, Mendis P, Foliente G. Embodied carbon analysis and benchmarking emissions of high and ultra-high strength concrete using machine learning algorithms. J Clean Prod 2020;262:121281. https://doi.org/10.1016/j.jclepro.2020.121281.

[59] Singh A. Experimental Study on Mechanical Properties of High Strength Glass Fiber Reinforced Light Weight Aggregate Concrete. Int J Mod Trends Sci Technol 2021;7:28–38. https://doi.org/10.46501/IJMTST0705004.

[60] Nath P, Sarker PK. Effect of GGBFS on setting, workability and early strength properties of fly ash geopolymer concrete cured in ambient condition. Constr Build Mater 2014. https://doi.org/10.1016/j.conbuildmat.2014.05.080.

[61] Adetukasi AO, Fadugba OG, Adebakin IH, Omokungbe O. Strength characteristics of fibre-reinforced concrete containing nanosilica. Mater Today Proc 2021. https://doi.org/10.1016/j.matpr.2020.03.123.

[62] Sankaranarayannan SS, Jagadesan JR. Comparison of high performance fly ash concrete using nano silica fume on different mixes. Circuits Syst 2016. https://doi.org/10.4236/cs.2016.78110.

[63] Yum WS, Yu J, Jeon D, Song H, Sim S, Kim DH, et al. Mechanical and durability properties of cementless concretes made using three types of cao-activated GGBFS binders. Materials 2022. https://doi.org/10.3390/ma15010271.

[64] Hameed MM, AlOmar MK, Baniya WJ, AlSaadi MA. Prediction of high-strength concrete: high-order response surface methodology modeling approach. Eng Comput 2022. https://doi.org/10.1007/s00366-021-01284-z.

[65] Jayasinghe A, Orr J, Ibell T, Boshoff WP. Minimising embodied carbon in reinforced concrete flat slabs through parametric design. J Build Eng 2022;50. https://doi.org/10.1016/j.jobe.2022.104136.

[66] Jhatial AA, Goh WI, Mastoi AK, Rahman AF, Kamaruddin S. Thermo-mechanical properties and sustainability analysis of newly developed eco-friendly structural foamed concrete by reusing palm oil fuel ash and eggshell powder as supplementary cementitious materials. Environ Sci Pollut Res 2021. https://doi.org/10.1007/s11356-021-13435-2.

[67] Kumar Karri S. Strength and Durability Studies on GGBS Concrete. Int J Civ Eng 2015. https://doi.org/10.14445/23488352/ijce-v2i10p106.

[68] Kattoli R, Briijbhushan S, Maneeth PD, Reddy SS, Siddharth B. Effect of partial replacement of cement by ground granulated blast furnace slag and sand by iron ore tailings on properties of concrete. Int J Adv Technol Eng Explor 2018. https://doi.org/10.19101/ijatee.2018.545008.

[69] Tawfik TA, Abd EL-Aziz MA, Abd El-Aleem S, Serag Faried A. Influence of nanoparticles on mechanical and nondestructive properties of high-performance concrete. J Chin Adv Mater Soc 2018. https://doi.org/10.1080/22243682.2018.1489303.

[70] Priyadarshana Thushara, Dissanayake Ranjith, Mendis Priyan. Effects of nano silica, micro silica, fly ash and bottom ash on compressive strength of concrete. J Civ Eng Arch 2015. https://doi.org/10.17265/1934-7359/2015.10.002.

[71] Lin Q, Chen Y, Liu C. Mechanical properties of circular nano-silica concrete filled stainless steel tube stub columns after being exposed to freezing and thawing. Nanotechnol Rev 2019. https://doi.org/10.1515/ntrev-2019-0053.

[72] Habibi A, Ramezanianpour AM, Mahdikhani M, Bamshad O. RSM-based evaluation of mechanical and durability properties of recycled aggregate concrete containing GGBFS and silica fume. Constr Build Mater 2021. https://doi.org/10.1016/j.conbuildmat.2020.121431.

[73] de la Rosa Á, Ruiz G, Poveda E. Study of the compression behavior of steel-fiber reinforced concrete by means of the response surface methodology. Appl Sci 2019. https://doi.org/10.3390/app9245330.

[74] Jayasinghe A, Orr J, Ibell T, Boshoff WP. Minimising embodied carbon in reinforced concrete beams. Eng Struct 2021. https://doi.org/10.1016/j.engstruct.2021.112590.

[75] Yu J, Mishra DK, Hu C, Leung CKY, Shah SP. Mechanical, environmental and economic performance of sustainable Grade 45 concrete with ultrahigh-volume Limestone-Calcined Clay (LCC). Resour Conserv Recycl 2021. https://doi.org/10.1016/j.resconrec.2021.105846.

[76] Lal Jain K, Singh Rajawat L, Sancheti G. Mechanical properties of ground granulated blast furnace slag made concrete. IOP Conf Ser Earth Environ Sci 2021. https://doi.org/10.1088/1755-1315/796/1/012063.

[77] Bautista-Gutierrez KP, Herrera-May AL, Santamaría-López JM, Honorato-Moreno A, Zamora-Castro SA. Recent progress in nanomaterials for modern concrete infrastructure: advantages and challenges. Materials 2019. https://doi.org/10.3390/ma12213548.

[78] Rezania M, Panahandeh M, Razavi SMJ, Berto F. Experimental study of the simultaneous effect of nano-silica and nano-carbon black on permeability and mechanical properties of the concrete. Theor Appl Fract Mech 2019. https://doi.org/10.1016/j.tafmec.2019.102391.

[79] Alqamish HH, Al-Tamimi AK. Development and evaluation of nano-silica sustainable concrete. Appl Sci 2021. https://doi.org/10.3390/app11073041.

[80] Kumar G, Mishra SS. Effect of ggbfs on workability and strength of alkali-activated geopolymer concrete. Civ Eng J 2021. https://doi.org/10.28991/cej-2021-03091708.

[81] Rahim NI, Mohammed BS, Abdulkadir I, Dahim M. Effect of crumb rubber, fly ash, and nanosilica on the properties of self-compacting concrete using response surface methodology. Materials 2022;15. https://doi.org/10.3390/ma15041501.

[82] Gomathi P, Sivakumar A. Synthesis of geopolymer based class-F fly ash aggregates and its composite properties in Concrete. Arch Civ Eng 2014. https://doi.org/10.2478/ace-2014-0003.

[83] Ferreira FPV, Tsavdaridis KD, Martins CH, De Nardin S. Steel-concrete-composite beams with precast hollow-core slabs: A sustainable solution. Sustainabililty 2021. https://doi.org/10.3390/su13084230.

[84] Said A. Beneficial use of nano-silica in concrete: a review. Trends Civ Eng Arch 2018. https://doi.org/10.32474/tceia.2018.01.000105.

[85] Fikri H, Krisologus YP, Permana R, Raafidiani R. Cyclic behavior of ground granulated blast furnace slag (GGBFS) concrete beams. IOP Conf Ser Mater Sci Eng 2020. https://doi.org/10.1088/1757-899X/830/2/022055.

[86] Rahman* I, Dev N. High strength nano silica based concrete. Int J Innov Technol Explor Eng 2020. https://doi.org/10.35940/ijitee.f4166.059720.

[87] Adamu M, Trabanpruek P, Jongvivatsakul P, Likitlersuang S, Iwanami M. Mechanical performance and optimization of high-volume fly ash concrete containing plastic wastes and graphene nanoplatelets using response surface methodology. Constr Build Mater 2021. https://doi.org/10.1016/j.conbuildmat.2021.125085.

[88] Jayasinghe A, Orr J, Ibell T, Boshoff WP. Comparing the embodied carbon and cost of concrete floor solutions. J Clean Prod 2021. https://doi.org/10.1016/j.jclepro.2021.129268.
[89] Rasin FA, Abbas LK, Kadhim MJ. Study the effect of nano materials addition on some properties of cement mortar. J Eng Sustain Dev 2017.
[90] Elrahman MA, Chung SY, Sikora P, Rucinska T, Stephan D. Influence of nanosilica on mechanical properties, sorptivity, and microstructure of lightweight concrete. Materials 2019. https://doi.org/10.3390/ma12193078.
[91] Chohan IM, Ahmad A, Sallih N, Bheel N, Ali M, Deifalla AF. A review on life cycle assessment of different pipeline materials. Results Eng 2023;19. https://doi.org/10.1016/j.rineng.2023.101325.
[92] Shi Y, Long G, Ma C, Xie Y, He J. Design and preparation of ultra-high performance concrete with low environmental impact. J Clean Prod 2019. https://doi.org/10.1016/j.jclepro.2018.12.318.
[93] Tugrul Tunc E, Alyamac KE. Determination of the relationship between the Los Angeles abrasion values of aggregates and concrete strength using the response surface methodology. Constr Build Mater 2020. https://doi.org/10.1016/j.conbuildmat.2020.119850.
[94] Hart J, D'Amico B, Pomponi F. Whole-life embodied carbon in multistory buildings: Steel, concrete and timber structures. J Ind Ecol 2021. https://doi.org/10.1111/jiec.13139.
[95] Bhardwaj B, Kumar P. Comparative study of geopolymer and alkali activated slag concrete comprising waste foundry sand. Constr Build Mater 2019. https://doi.org/10.1016/j.conbuildmat.2019.03.107.
[96] Robati M, Oldfield P. The embodied carbon of mass timber and concrete buildings in Australia: An uncertainty analysis. Build Environ 2022. https://doi.org/10.1016/j.buildenv.2022.108944.
[97] Zhu Q. CO2 abatement in the cement industry Industry. IEA Clean Coal Centre 2011:121–127.
[98] Marceau M.L., Nisbet M.A., VanGeem M.G. Life Cycle Inventory of Portland Cement Concrete. SN3011, Portl Cem Assoc Skokie, Illinois, PCA 2007.
[99] Turner LK, Collins FG. Carbon dioxide equivalent (CO_2-e) emissions: a comparison between geopolymer and OPC cement concrete. Constr Build Mater 2013;43:125–30. https://doi.org/10.1016/j.conbuildmat.2013.01.023.
[100] Jones R., Mccarthy M., Newlands M. Fly Ash Route to Low Embodied CO 2 and Implications for Concrete Construction. World Coal Ash Conf 2011.
[101] Kumar R, Shafiq N, Kumar A, Jhatial AA. Investigating embodied carbon, mechanical properties, and durability of high-performance concrete using ternary and quaternary blends of metakaolin, nano-silica, and fly ash. Environ Sci Pollut Res 2021;28:49074–88. https://doi.org/10.1007/s11356-021-13918-2.
[102] Adamu M, Mohammed BS, Shahir Liew M. Mechanical properties and performance of high volume fly ash roller compacted concrete containing crumb rubber and nano silica. Constr Build Mater 2018;171:521–38. https://doi.org/10.1016/j.conbuildmat.2018.03.138.
[103] Yang K., Song J., Production KS-J of C, 2013 U. Assessment of CO2 reduction of alkali-activated concrete. Elsevier 2013.
[104] Bheel N, Ali MOA, Tafsirojjaman, Khahro SH, Keerio MA. Experimental study on fresh, mechanical properties and embodied carbon of concrete blended with sugarcane bagasse ash, metakaolin, and millet husk ash as ternary cementitious material. Environ Sci Pollut Res 2022;29:5224–39. https://doi.org/10.1007/s11356-021-15954-4.
[105] Bheel N, Benjeddou O, Almujibah HR, Abbasi SA, Sohu S, Ahmad M, et al. Effect of calcined clay and marble dust powder as cementitious material on the mechanical properties and embodied carbon of high strength concrete by using RSM-based modelling. Heliyon 2023;9. https://doi.org/10.1016/j.heliyon.2023.e15029.
[106] Birniwa AH, Mohammad REA, Ali M, Rehman MF, Abdullahi SS, Eldin SM, et al. Synthesis of Gum Arabic Magnetic Nanoparticles for Adsorptive Removal of Ciprofloxacin: Equilibrium, Kinetic, Thermodynamics Studies, and Optimization by Response Surface Methodology. Separations 2022;9. https://doi.org/10.3390/separations9100322.
[107] Ali M, Kumar A, Yvaz A, Salah B. Central composite design application in the optimization of the effect of pumice stone on lightweight concrete properties using RSM. Case Stud Constr Mater 2023;18. https://doi.org/10.1016/j.cscm.2023.e01958.
[108] Ali M, Khan MI, Masood F, Alsulami BT, Bouallegue B, Nawaz R, et al. Central composite design application in the optimization of the effect of waste foundry sand on concrete properties using RSM. Structures 2022;46:1581–94. https://doi.org/10.1016/j.istruc.2022.11.013.
[109] Adamu M, Haruna SI, Ibrahim YE, Alanazi H. Investigating the properties of roller-compacted rubberized concrete modified with nanosilica using response surface methodology. Innov Infrastruct Solut 2022. https://doi.org/10.1007/s41062-021-00717-4.
[110] Rooholamini H, Hassani A, Aliha MRM. Evaluating the effect of macro-synthetic fibre on the mechanical properties of roller-compacted concrete pavement using response surface methodology. Constr Build Mater 2018. https://doi.org/10.1016/j.conbuildmat.2017.11.002.
[111] Bheel N, Khoso S, Baloch MH, Benjeddou O, Alwetaishi M. Use of waste recycling coal bottom ash and sugarcane bagasse ash as cement and sand replacement material to produce sustainable concrete. Environ Sci Pollut Res 2022;29:52399–411. https://doi.org/10.1007/s11356-022-19478-3.
[112] MPA The Concrete Centre. Comparison of embodied carbon in concrete structural systems. 2022.